Technical Report

TR-99-36

Uranium transport around the reacator zone at Okelobondo (Oklo)

Data evaluation with M3 and HYTEC

I Gurban, M Laaksoharju
INTERA KB, Stockholm

B Made, E Ledoux
Ecole des Mines, Paris

December 1999

Svensk Kärnbränslehantering AB
Swedish Nuclear Fuel
and Waste Management Co
Box 5864
SE-102 40 Stockholm Sweden
Tel 08-459 84 00
+46 8 459 84 00
Fax 08-661 57 19
+46 8 661 57 19

Uranium transport around the reacator zone at Okelobondo (Oklo)

Data evaluation with M3 and HYTEC

I Gurban, M Laaksoharju
INTERA KB, Stockholm

B Made, E Ledoux
Ecole des Mines, Paris

December 1999

Keywords: Natural Analogue, Coupled Code, Statistical-Mathematical Code, Data Evaluation, Site Investigation, Uranium Transport, Hydrodynamic and Geochemical Modelling

ABSTRACT

The Swedish Nuclear Fuel and Waste Management Company (SKB) is conducting and participating in Natural Analogue activities as part of various studies regarding the final disposal of high level nuclear waste (HLW). The aim of this study is to use the hydrogeological and hydrochemical data from Okélobondo (Oklo Natural Analogue) to compare the outcome of two independent modelling approaches (HYTEC and M3). The modelling helps to evaluate the processes associated with nuclear natural reactors such as redox, adsorption/desorption and dissolution/precipitation of the uranium and to develop more realistic codes which can be used for site investigations and data evaluation.

HYTEC (1D and 2D) represents a deterministic, transport and multi-solutes reactive coupled code developed at Ecole des Mines de Paris. M3 (Multivariate Mixing and Mass balance calculations) is a mathematical-statistical concept code developed for SKB. M3 can relatively easily be used to calculate mixing portions and to identify sinks or sources of element concentrations that may exist in a geochemical system. M3 helped to address the reactions in the coupled code HYTEC. Thus, the major flow-paths and reaction paths were identified and used for transport evaluation.

The reactive transport results (one-dimensional and two-dimensional simulations) are in good agreement with the statistical approach using the M3 model. M3 and HYTEC show a dissolution of the uranium layer in contact with upwardly oxidising waters. M3 and HYTEC show a gain of manganese rich minerals downstream the reactor. A comparison of the U and Mn plots for M3 deviation and HYTEC results showed an almost mirror behaviour. The U transport stops when the Mn gain increases. Thus, HYTEC and M3 modelling predict that a possible reason for not having U transport up to the surface in Okélobondo is due to an inorganic trap which may hinder the uranium transport.

The two independent modelling approaches can be used to complement each other and to better understand the processes that can take place in nature. This provides the opportunity to assess the necessary tools for site investigations, data evaluation and helps to trace the reactions and to identify the hydro-geo-chemical system. Thus, we can build reliable tools which can be used to assess the performance of possible waste repository sites.

ABSTRACT (SWEDISH)

Svensk kärnbränslehantering (SKB) utför och deltar i undersökningar av naturliga analogier som en del i de omfattande studier angående slutförvar av använt kärnbränsle. Syftet med denna studie är att använda hydrogeologiska och hydrokemiska data från Okélobondo (Oklo Natural Analogue) för att jämföra resultatet av de två oberoende modellerna HYTEC och M3. Modelleringen hjälper att utvärdera de processer som är associerade med naturliga kärnreaktorer såsom redox, adsorption/desorption och upplösning/utfällning av uran. Den kan även vara en hjälp till att utveckla mer realistiska koder vilka kan användas vid platsundersökningar och vid utvärdering av data.

HYTEC (1D och 2D) representerar deterministiska transport och kemiskt reaktivt kopplade modeller utvecklade vid Ecole des Mines i Paris. M3 (kallad Multivariat Blandning och Massbalans beräkningar) är ett matematiskt-statistiskt koncept utvecklat för SKB. M3 kan relativt lätt användas för att identifiera tillskott eller förlust av elementhalter som kan förekomma i ett geokemiskt system. M3 kan bidra till att adressera de reaktioner som kan modelleras i den kopplade koden HYTEC. Resultatet är att de huvudsakliga flödesvägarna och reaktionsvägarna kan identifieras och användas för transportutvärdering.

Den reaktiva transportmodellen (endimensionella och tvådimensionella simuleringar med HYTEC) är i god överensstämmelse med det statistiska tillvägagångssättet som används i M3 modellen. HYTEC och M3 visar en upplösning av uran i kontakt med uppströms oxiderande vatten. HYTEC och M3 visar ett tillskott av manganrika mineral nedströms om reaktorn. HYTEC resultaten och M3 avvikelsen för uran och mangan uppvisar i stort sett samma mönster, transport av U hindras när tillskottet av Mn ökar. Följaktligen förutsäger HYTEC och M3 modelleringarna att en möjlig orsak för att inte ha transport av U upp till ytan i Okélobondo orsakas av en oorganisk fälla, vilken kan hindra urantransport.

De två oberoende modellerna kan användas för att komplettera varandra och för att ge en bättre förståelse av de processer som kan ske i naturen. Detta ger ett tillfälle att testa nödvändiga verktyg för platsundersökningar som kan vara till hjälp för att utvärdera data, spåra reaktioner och identifiera hydrogeokemiska system. Vi kan således bygga tillförlitliga verktyg som kan användas vid säkerhetsanalys av framtida slutförvarsplatser.

CONTENTS

LIST OF FIGURES

1 INTRODUCTION

The Swedish Nuclear Fuel and Waste Management Company (SKB) is responsible for the safe handling and disposal of nuclear wastes in Sweden. This responsibility includes conducting studies into the siting of a deep repository for high-level nuclear waste. This report compares two different modelling approaches as part of a performance assessment (PA) study of the long-term safety of a natural repository at Okélobondo (Oklo) in Gabon.

SKB is conducting and participating in Natural Analogue activities as part of various studies regarding the final disposal of high level nuclear waste (HLW). The aim of this study is to use the hydrogeological and hydrochemical data from Oklo Natural Analogue to compare the outcome of two independent modelling approaches which can be used to predict the repository performance over long periods of time.

The Oklo site is a unique analogue for the source term such as uraninite versus spent fuel and the engineered and geological barriers (clay minerals, apatite). This provides an opportunity to assess the necessary tools for future performance assessment of the prospective real waste repository sites.

2 PROJECT DESCRIPTION

2.1 PROJECT DESCRIPTION

The work described in this study is a collaboration between Ecole des Mines de Paris and Intera KB. The study describes the continued work at the Bangombé site (Oklo) (Gurban *et al*, 1998).

The natural analogue project in Okélobondo concerns groundwater modelling based on existing data. The aim is to use different computer methodologies to characterise the evolution of the groundwater system and its implications in radionuclide transport, and then to compare and integrate the results within a performance assessment concept concerning uranium transport from the source to the biosphere. Thus, the modelling helps to evaluate the processes associated with nuclear natural reactors such as redox, adsorption/desorption and dissolution/precipitation of the uranium and to develop more realistic codes used in performance assessment studies.

3 TOOLS

Two approaches were used: a classic one, representing a coupled hydro-geo-chemical transport code developed at Ecole des Mines de Paris named HYTEC 1D and 2D and a new concept code named M3 developed for SKB. The M3 results are visualised using the Voxel Analyst code and the outcome of the uranium transport predictions are made from a performance assessment point of view.

3.1 HYTEC2D DESCRIPTION

The 2D, deterministic, transport and multi-solutes reactive code named HYTEC-2D (Salignac, 1997 and 1998) is the result of combining the solute transport code METIS (Cordier and Goblet 1996, Goblet 1981) and the chemical speciation code CHESS (van der Lee, 1997 and 1999) developed at Ecole des Mines. It allows the computation of the chemical composition of the groundwater through a heterogeneous geological system taking into account the interaction between fluid and rock due to precipitation-dissolution, gas formation, ion exchange, and surface complexation. The results are expressed in terms of distribution in space and time of the aqueous, solid or gaseous species, of the saturation index versus minerals that may control the geological system and of the mass balance between fluid, solid and gas. Several hypotheses for the control of dissolved uranium can thus be tested and compared to the experimental database.

These results were then compared to the M3 analysis results expressing the chemical tendencies.

3.2 M3 DESCRIPTION

The origin and evolution of the groundwater can be described if the effect from mixing and reactions can be examined separately. In order to do this separation a new method named Multivariate Mixing and Mass balance calculations (abbreviated to M3) was constructed (Laaksoharju *et al.*, 1997 and 1998). The model consists of 3 steps where the first step is a standard principal component analysis, followed by mixing, and finally by mass balance calculations. Mass balance calculations are used to define the sources and sinks for different elements, which deviate from the ideal mixing model used in the mixing calculations. The mixing portions are used to predict new values for the elements. No deviation from the measured value indicates that mixing can explain the element behaviour. A source or sink is due to mass balance reactions. M3 uses the opposite approach to that of other standard methodologies. In M3 the mixing processes are evaluated and calculated first. The constituents that cannot be described by mixing are described by reactions. M3 computer code determines the origin of the water, the mixing proportions and the most important mass balance reactions that take place in the groundwater.

3.3 VOXEL ANALYST

In order to visualise the M3 results, the Voxel Analyst computer code was used. Voxel Analyst is a general-purpose data visualisation and analysis tool that helps to understand the relationship between different attributes within a 3-dimensional volume data set. The major flow-paths and reaction paths were identified and used for transport evaluation.

4 SITE PRESENTATION

A geological cross-section CD was produced based on the collected data. This was used as a basis for the local-scale modelling (Gurban, 1996). The model domain corresponds to a vertical cross-section between OK2 and SA992 and through the reactor OK84, within the CD profile (figure 4-1). The lower boundary of the model is located at -34 m below sea level while the upper one varies with the topography between 440 m and 377 m above sea level. The coordinates of the boreholes are listed in Appendix 1.

The uranium deposit is located at a depth of about 300m, and is affected by oxidation/dissolution processes which also precipitate UO_2 bearing minerals. The domain of this study has been represented by two geological sections N-S and NW-SE, which include the OK84 reactor (see Blind Prediction Modelling Exercise; Bruno *et al.*, 1997). Geographically, the higher areas are located in the Massango Plateau, whereas the natural drainage area is the valley of the Mitembé river. The OK84 uranium reactor is situated close to a fault zone, which separates the plutonic basement from the Franceville sedimentary series. The sedimentary materials are made up of FA sandstone and FB pelites with some interbedded sandy-dolomitic bodies called "Complexes". In the upper outcropping FB series in the Massango Plateau, there are some economically important manganese-rich black pelites. Finally, a superficial lateritic soil, a few metres thick, is developing (Salas *et al.*, 1998). The hydrodynamic boundary conditions are extracted from Gurban *et al.* (figure 4-2).

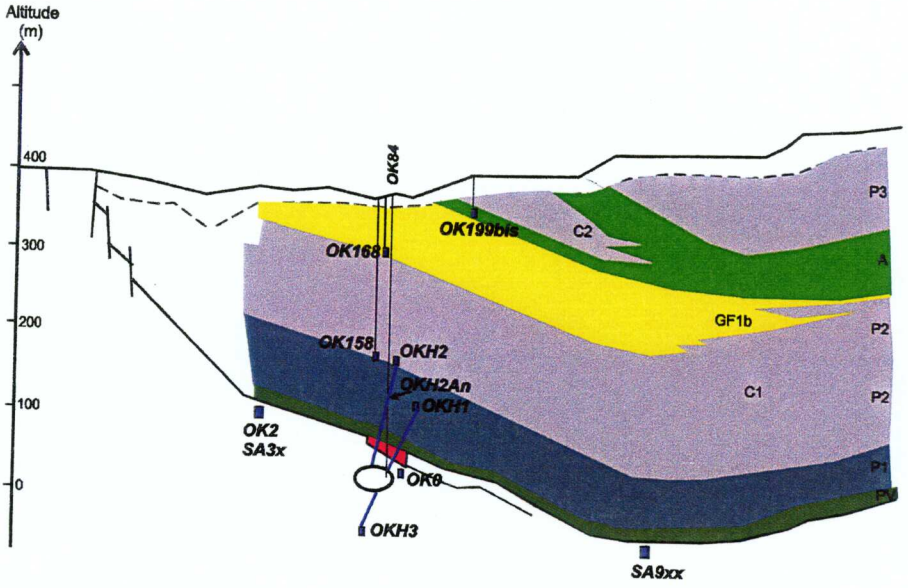

Figure 4-1 Geological profile (CD) at the Okélobondo site (Oklo, Gabon). (1) Pelites (P1, P2, P3, PV and Ampelites); (2) Complexes (C1, C2, GF1b); (3) Uranium Deposit and (4) Sandstones FA.

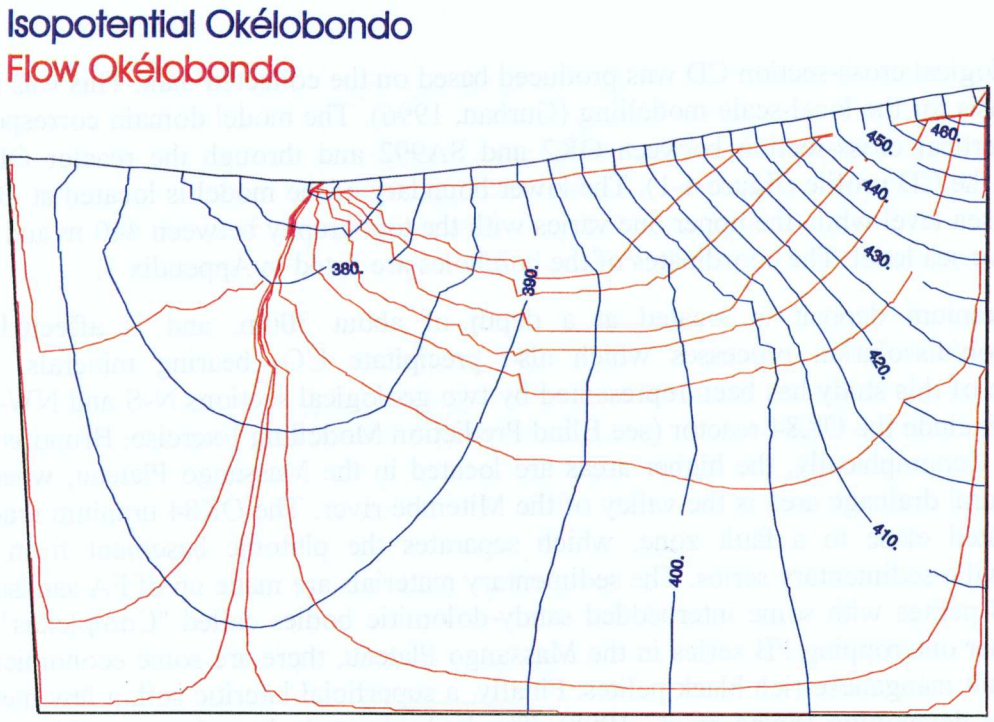

Figure 4-2 Isopotential and flow map, from Gurban et al. 1996, showing the major flow paths (in red) at the Okélobondo site.

5 HYTEC MODELLING

5.1 HYTEC APPROACH

One modelling aim of this study is to describe the geochemical uranium behaviour around the Okélobondo mine using the reactive transport code HYTEC (-1D and -2D). Two major mechanisms take place in the aquifer: transport due to advection, diffusion and dispersion as well as chemical reactions into the aqueous phase and at the interface of the solid matrix.

Each of these mechanisms is complex enough to require numerical models. Ecole des Mines has developed a speciation static code CHESS (van der Lee, 1999) for the modelling of the geochemistry, and the code METIS (Cordier and Goblet, 1996) for the transport. Combining the two codes, Ecole des Mines obtained a transport multi-solute reactive code named HYTEC-2D (Salignac 1998). This code works in heterogeneous saturated media and allows the hydrodynamic parameters and the chemical conditions defining the system to regionalise. This code is based on the algorithm named "two-steps" iteractive. It means that the chemical and transport calculations are made sequentially by two distinct models.

a) The *chemical model CHESS* enables the speciation within a geochemical system in the hypothesis of local chemical equilibrum to be calculated using the thermodynamic constants of the assumed reactions. It takes into consideration the method of the base components, considering the system as a vectorial space where a base is chosen. If species (N_{es}) are correlated by independent reactions (N_r), is defined $N_{co}= N_{es}-N_r$, named base components and represents the unknowns. To solve the N_{co} equations system, the action mass law and conservative mass balance law are used.The resulting equations are strongly non-linear. The iterative Newton Raphson method is used to solve them.

b) The *hydrodynamic model METIS* enables a steady state flow to be calculated and combined with a transient transport of chemical species, in a saturated, monophasic and bidimensional medium.

c) HYTEC-2D combination

The two systems of equations are very different:

- The chemical equations are independent in space (the speciation is calculated step by step), and the transport equations are solved simultaneously in all the domains.
- The chemical equations are solved for all the base components simutaneously, but the transport equations are independent in this respect.
- The chemistry is not dependent on time (local equilibrium), but the transport is dependent on time. In HYTEC-1D code (Van der Lee, 1997), kinetic of reactions are taken into account.

The numerical solution method of the coupled geochemistry-transport model, HYTEC-2D, includes a two-step iterative sequence where the first step is the speciation calculation on all the elements of the domain and the second step is the solute transport calculation, for each time step. As local equilibrium is assumed, the chemical reactions are instantaneous. Only the base components are transported. The concentrations of the secondary species are known at each step from the speciation calculations. The transport equation used here is that of advection-diffusion, using the total concentration of the components as a variable and representing changes (gains or losses), during a time step, for the relevant solute species. This two-step approach is iterative in that, at the end of the transport step, a check can be done to ensure that the condition of equilibrium at all points is always respected.

5.2 MODELLED AREA

A 2D section of 1,000 x 500 m NW-SE including the OK84 uranium ore body has been selected for HYTEC-2D modelling (Gurban, 1996). The 2D space is discretised into 1254 nodes and 1176 quadrangle elements of variable area. The conceptual hydrogeochemical model is based on a local flux model defined in preceding studies (Gurban *et al.*, 1992-1996).

5.3 HYTEC MODELLING SETTINGS

5.3.1 Hydrogeological model

The hydrodynamical model describes the existence of two convective cells formed by a topography-driven flow. One convective cell is located to the west of the Mitembé river, which mainly drains the FA sandstone, and the other cell is located to the east of the river, which crosses the FB pelites, the dolomitic complexes and the FA sandstone. The system was divided into six different lithological domains (figure 4-1): FB-pelites, FB-Complexes, manganiferous pelites, the uranium deposit with the reaction zone OK84, FA-sandstone and a basement fault area. The hydrogeological properties and initial mineralogical compositions of these domains are described in Gurban (1996) and Salas *et al.* (1998). The residence time of the water in the system is approximately 15,000 years. An one dimensional approach has been carried out along a flow line of the convective cells defined by the 2D hydrogeological model (Gurban, 1996). This geochemical system is showed by the mineralogical description of a column in figure 5-1.

The boundary conditions are as follows:

No flow condition is prescribed on the left and right sides of the domain as well as at the bottom of the cross-section.

Prescribed heads are equal with the topographic elevation on the line of nodes representing the soil surface.

Figure 4-2 shows the stream lines generated by these geological and boundary conditions.

Physical parameters

- Porosity: constant and uniform, 1 %.

- Longitudinal and transversal dispersivities and the diffusion

coefficient are constant and uniform, equal to 5m, 2m and $10^{-7}m^2/s$.

- Permeability:

$K_{x,y} = 10^{-8}$m/s for the complexes and F1b sandstone

$K_{x,y} = 10^{-9}$ m/s for the pelites

$K_{x,y} = 10^{-6}$ m/s cover

$K_{x,y} = 10^{-10}$ m/s FA sandstones

$K_{x,y} = 10^{-8}$ m/s bedrock fault

5.3.2 Chemical composition of the groundwater

From the analyses of water collected from several boreholes in the area (see Blind Prediction Modelling Exercise; Bruno *et al.*, 1997) two types of groundwater were distinguished in a pH-pE diagram (Salas *et al.*, 1998):

Type I is common in many ground water environments (such as Bangombé), whose hydrochemistry is controlled by the redox equilibrium Fe^{2+}-$Fe(OH)_3$. There are two subgroups:

a) Type I-a has neutral to basic pH and reducing conditions; they show saturation with respect to uraninite. The samples are taken from boreholes drilled in the complexes and in the upper formations.

b) Type I-b waters has more oxidising conditions, neutral to slightly acidic, and subsaturated with respect to uraninite. They are taken from boreholes drilled from galleries in FA sandstones.

Type II are oxidising and slightly basic ground waters, subsaturated with respect to uraninite. They come from boreholes drilled in galleries excavated horizontally around the ore body in the FA sandstones and in the base of FB pelites. Moreover, the two water types described above are also distinct with respect to the Fe/Mn ratio.

Type I waters generally have a Fe/Mn ratio greater than 1, whereas Type II waters commonly have a Fe/Mn ratio of less than 1. It appears that the Fe^{2+}-$Fe(OH)_3$ may have an important role in controlling the chemistry of Type I waters. Manganese minerals play a significant role in controlling the chemistry of Type II waters.

5.3.3 Description of the geochemical system

139 chemical species and 71 minerals were generated from 14 base components (H^+, Ca^{2+}, Na^+, K^+, Mg^{2+}, Al^{3+}, UO_2^{2+}, Fe^{2+}, Mn^{2+}, Cl^-, HCO_3^-, $SiO_2(aq)$ and $O_2(aq)$). The aqueous complexation reactions, redox reactions and precipitation/dissolution reactions were particularly investigated in order to describe aqueous solutions in the Okélobondo system. The mineralogical composition of the aquifer lithologies has been done with the following basic minerals: illite, daphnite-14A, $Fe(OH)_3$, kaolinite, dolomite, calcite, rhodochrosite, manganite, hausmannite, quartz, chalcedony and uraninite, all of whose equilibrium constants, apart from illite (Gurban *et al.*, 1996), were those included in the HYTEC-1D / HYTEC-2D (LLNL database) obtained from CISSFIT calculation method.

Four distinctive zones (figure 4-1) define the geochemical system (March 1993 campaign for the groundwater aqueous composition): Sandstone-FA / OKH3 groundwater; Complexes - Sandstone-FB / OK199bis groundwater; Pelites (P1, P2, P3 units and Ampelites) / OK158 groundwater; Reactor and Uranium Deposit / OKH2An groundwater.

Sandstone-FA

Mineralogy: The minerals describing this zone at the Okélobondo site are quartz (95%) and daphnite-14A (5%).

Groundwater: The groundwater in borehole OKH3 gives the chemical composition of the aqueous solution (pH = 7.56, Eh = 445 mV). This groundwater is over-saturated with respect to ferric minerals (ferrihydrite, magnetite); U(VI) minerals (haiweeite), clay minerals (kaolinite, muscovite, illite, beidellite), microcline, calcite and dolomite, quartz and chalcedony. The final thermodynamic equilibrium calculated with the CHESS code (van der Lee, 1999) is: calcite-dolomite-quartz-kaolinite and ferrihydrite. The SI of uraninite, coffinite and haiweeite is -14.5, -14.9 and -1.3, respectively.

Complexes - Sandstone-FB

Mineralogy: Illite (30%), dolomite (30%), chalcedony (30%), daphnite (7%) and K-feldspar (3%) are the major minerals characterising this unit.

Groundwater: Groundwater in the borehole OK199bis can describe the chemical composition of the aqueous solution (pH = 6.66; Eh = 94 mV) which is over-saturated with respect to ferric minerals (magnetite, cronstedtite-7A), clay minerals (illite, muscovite, beidellite-Mg, kaolinite, gibbsite, smectite-low-Fe-Mg), quartz and chalcedony. The stable mineralogical system calculated is defined by quartz-kaolinite-magnetite. The saturation index of uranium minerals - uraninite, coffinite and schoepite - is equal to -2.1, -2.9 and -4.3, respectively.

Pelites (P1, P2, P3 units and Ampelites)

Mineralogy: The solid phases describing these units are illite (63%), chalcedony (20%), daphnite (13%) and K-feldspar (4%) as well as minor minerals such as ferrihydrite, manganite, rhodocrosite and calcite.

Groundwater: The chemical composition of the aqueous solution is given by the groundwater in borehole OK158 (pH = 7.2, Eh = 23 mV) which is over-saturated with respect to clay minerals (illite, muscovite, kaolinite, beidellite), ferric minerals (magnetite, cronstedtite-7A), K-feldspar, quartz and chalcedony. The final thermodynamic equilibrium calculated is defined by the quartz-magnetite-illite system. The saturation index with respect to uraninite, coffinite and schoepite is -1.0, -1.8 and -4.5, respectively.

Reactor and Uranium Deposit

Mineralogy: Uraninite (66%), "argile de pile" ("illite de pile", 31%) and daphnite-14A (3%) are the minerals describing this unit on the Okélobondo site. Minor minerals are ferrihydrite and chalcedony.

Groundwater: The chemical composition of the aqueous solution in the reactor and uranium deposit zone is given by the groundwater in borehole OKH2An (pH = 8.59, Eh = 293 mV). Ferric minerals (magnetite, cronsteditite-7A, ferrihydrite), calcite and dolomite are minerals in over-saturation. The stable mineralogical system is given by calcite-dolomite-magnetite assemblage. The under-saturation of uranium minerals (SI uraninite = - 15.2, SI coffinite = -16.3; SI haiweeite = -10.3) in groundwater OKH2An are important and can be related to the oxygen contamination during sampling.

5.3.4 Reactive transport modelling

In contrast to the Bangombé site reactive transport modelling (Madé and Salignac, 1998, Madé *et al.*, 1998), no REDOX BUFFER ZONE (siderite/ferrihydrite equilibrium or organic matter) has been defined around the uranium deposit zone (and the reaction zone) to protect it from the oxidising dissolution.

Initial conditions

At the top of the section (-1D and -2D approaches), the water infiltrating in the area has a chemical composition of rain water as well as oxidising and acidic diluted aqueous solution (Eh = 880 mV; pH = 5.66 and $pCO_2 = 10^{-3.5}$). Six successive zones are defined in order to describe the hydro-geochemical system (figure 4-1 (2D approach); figure 5-1 (1D approach)) at Okélobondo site:

Manganese deposit zone characterised by manganite (MnO_2) and Rhodochrosite ($MnCO_3$) solid phases. The thermodynamic equilibrium between Mn^{3+} and Mn^{2+} minerals gives an Eh and a pH equal to 99 mV and 9.58, respectively. The total aqueous concentration calculated is equal to $2.301x10^{-5}$ mol/l for HCO_3^- and Mn^{2+}.

Pelite zone characterised by the mineralogical composition: chalcedony (200 mg/l); illite (630 mg/l); daphnite-14A (130 mg/l) and K-feldspar (40 mg/l) which controls the Eh and the pH value at -279 mV and 8.46, respectively. The aqueous concentrations of species are equal to $1.93x10^{-4}$ mole/l for $SiO_2(aq)$; $1.1x10^{-7}$ mole/l for Mg^{2+}; $5.93x10^{-6}$ mole/l for K^+; $1.80x10^{-7}$ mole/l for Al^{3+} and $5.53x10^{-8}$ mole/l for Fe^{2+}.

Complexes zone characterised by the following mineralogical composition : chalcedony (300 mg/l); dolomite (300 mg/l); illite (300 mg/l) and K-feldspar (30 mg/l). The values of Eh and pH are equal to 330 mV and 9.62, respectively. The aqueous concentrations of species are equal to $1.11x10^{-4}$ mole/l for HCO_3^-; $2.76x10^{-4}$ mole/l for SiO_2aq; $2.54x10^{-5}$ mole/l for Mg^{2+}; $2.29x10^{-7}$ mole/l for K^+; $8.79x10^{-7}$ mole/l for Al^{3+} and $5.53x10^{-5}$ mole/l for Ca^{2+}.

Green Pelites zone is formed by chalcedony (100 mg/l); illite (600 mg/l); daphnite-14A (250 mg/l) and K-feldspar (40 mg/l) with a pH equal to 8.46 and an Eh equal to -279 mV. The aqueous concentrations of species are equal to $1.93x10^{-4}$ mole/l for $SiO_2(aq)$; $1.1x10^{-7}$ mole/l for Mg^{2+}; $5.93x10^{-6}$ mole/l for K^+; $1.80x10^{-7}$ mole/l for Al^{3+} and $5.53x10^{-8}$ mole/l for Fe^{2+} as for the Pelites zone (2).

Uranium deposit zone is characterised by uraninite (660 mg/l) and "Illite de Pile" (310 mg/l) given that the pH and Eh values are equal to 6.91 and -99 mV, respectively. The aqueous concentrations of species are equal to $5.81x10^{-6}$ mole/l for SiO_2 (aq); $1.11x10^{-6}$ mole/l for Mg^{2+}; $2.67x10^{-6}$ mole/l for K^+; $5.35x10^{-6}$ mole/l for Al^{3+} and $3.92x10^{-10}$ mole/l for UO_2^{2+}.

Sandstone-FA zone characterised by quartz (950 mg/l) and daphnite-14A (100 mg/l) controls the pH and Eh values at 7.87 and -244 mV, respectively. The aqueous concentrations of species are equal to $1.89x10^{-4}$ mole/l for $SiO_2(aq)$; $4.58x10^{-8}$ mole/l for Al^{3+} and $7.96x10^{-7}$ mole/l for Fe^{2+}.

The initial geochemical conditions for the HYTEC-1D modelling approach are shown in figure 5-2 (pH, Eh, aqueous U, aqueous Mn and aqueous carbonates) and in figures 5-10 (Eh, pH), 5-11 (aqueous U) and 5-12 (aqueous Mn) for the HYTEC-2D modelling approach.

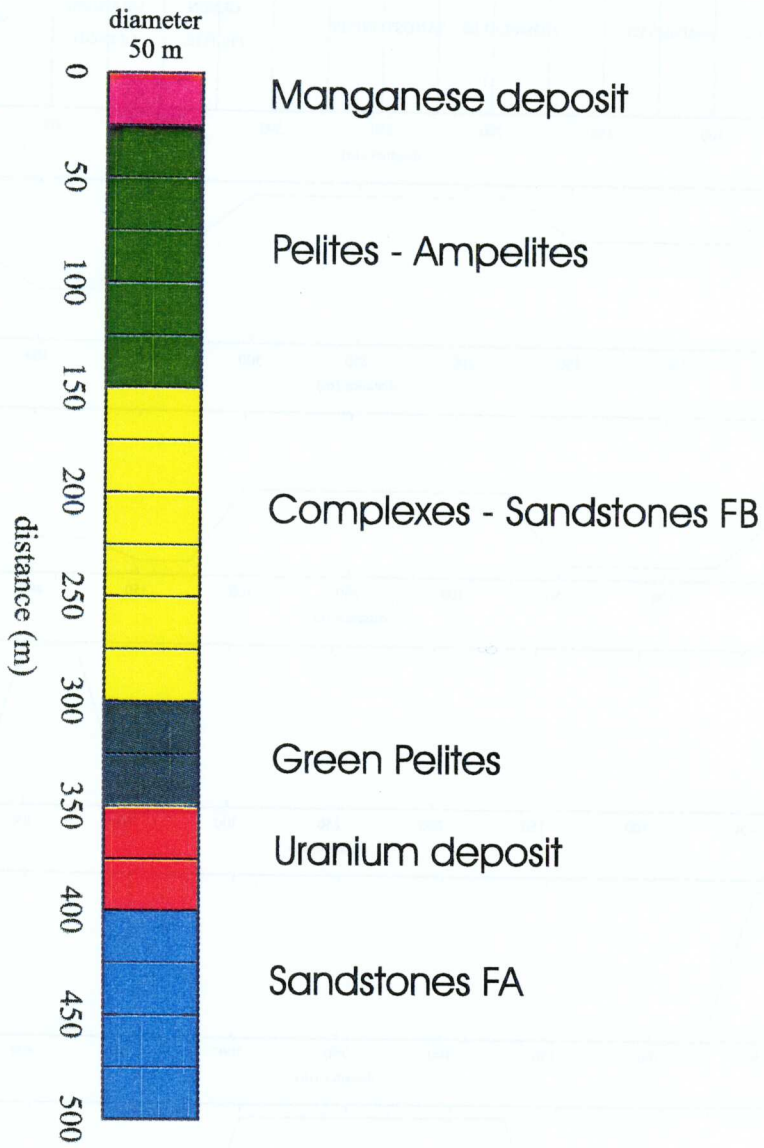

Figure 5-1 Conceptualisation of the Geochemical System for the HYTEC-1D Modelling along a flow line. The chemical composition of water at the top of the column is similar to a rain water (log PCO2(g) = -3.5; pH = 5.66; Eh = 880 mV.

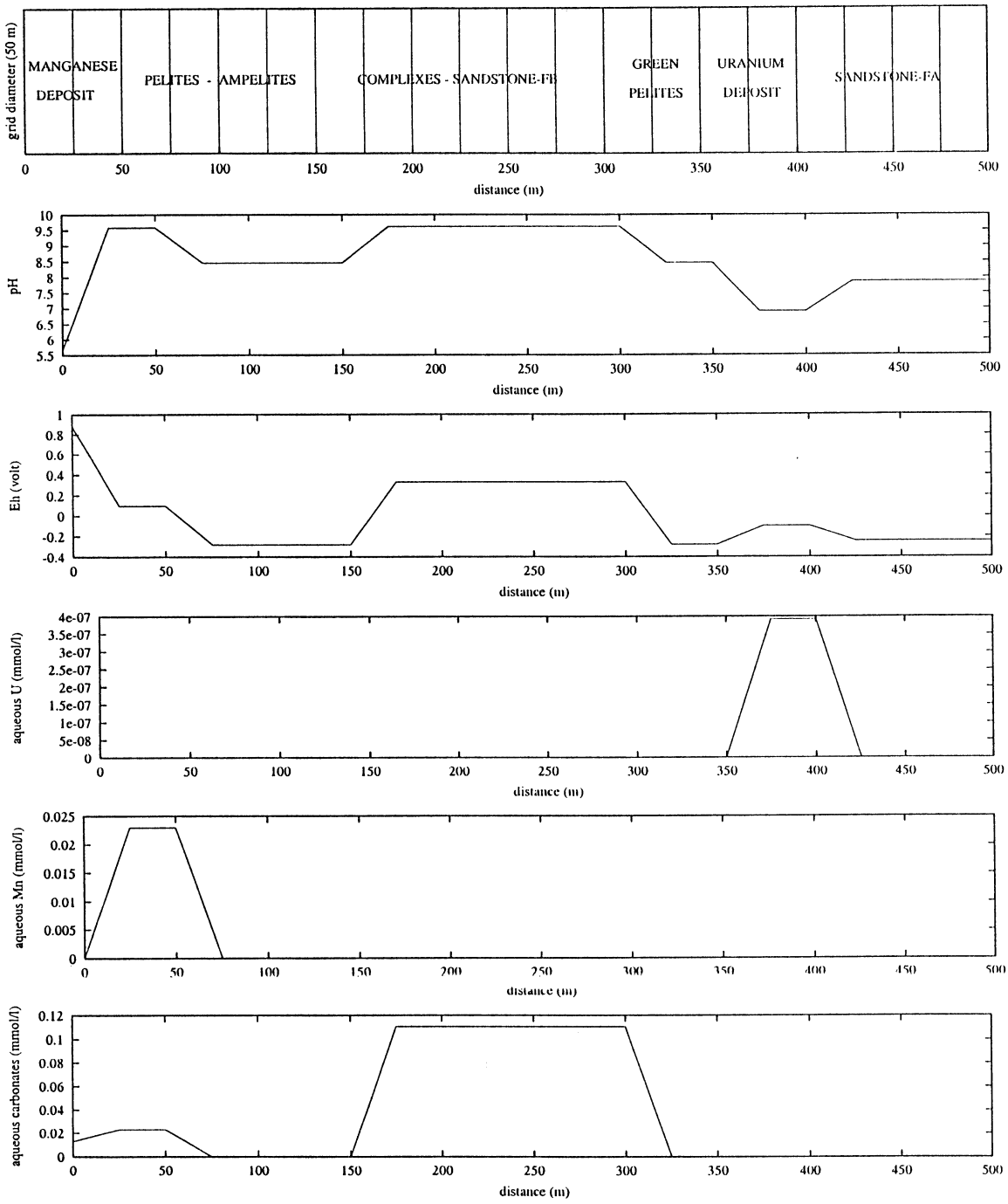

Figure 5-2 HYTEC-1D Modelling: initial geochemical conditions in the different mineralogical zones (pH, Eh, aqueous U, aqueous Mn and aqueous carbonates in mmol/l).

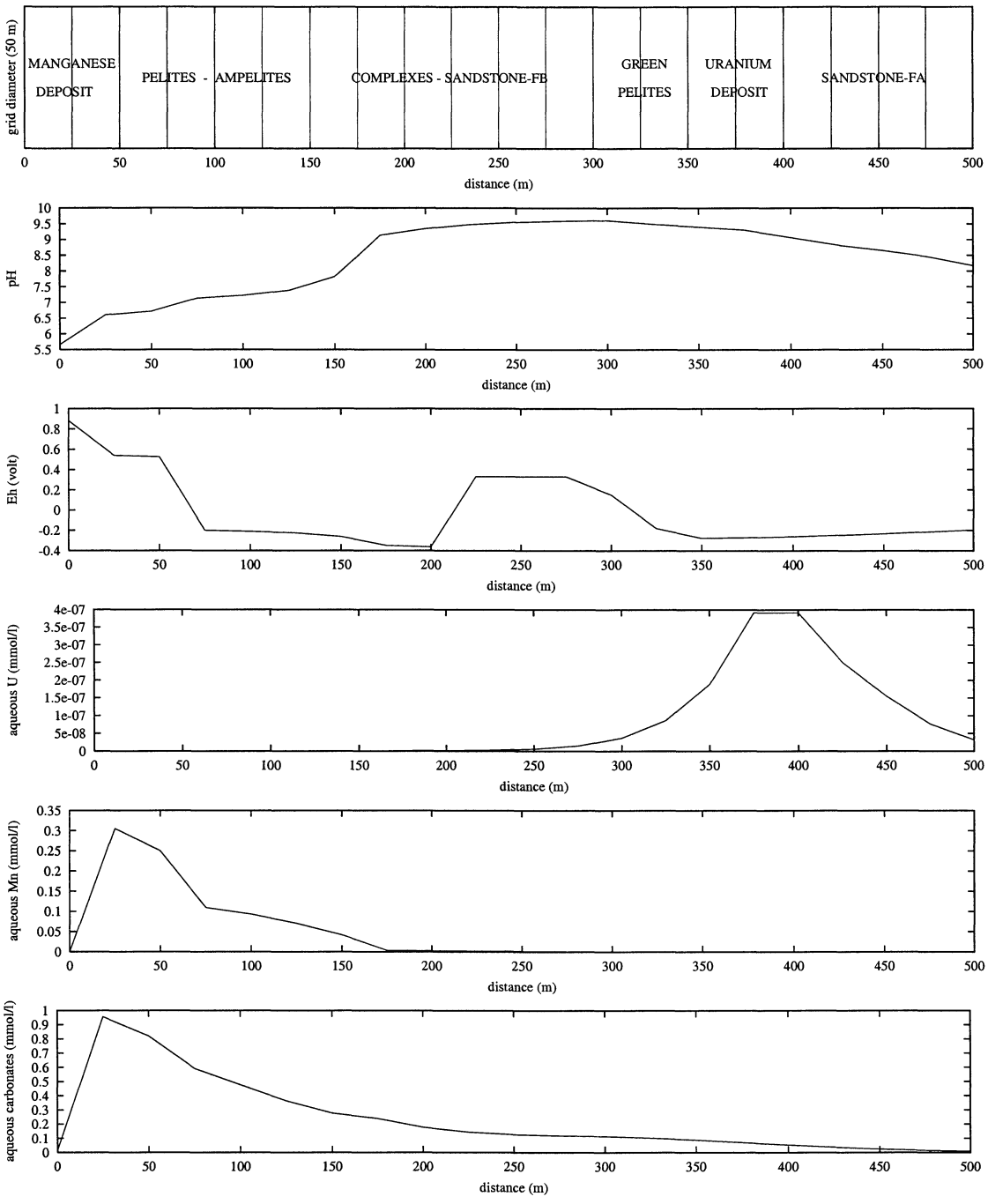

Figure 5-3 HYTEC-1D Modelling (time = 4 years): Evolution of pH and Eh values, aqueous concentrations of U, Mn and HCO_3^- in mmol/l along a flow line.

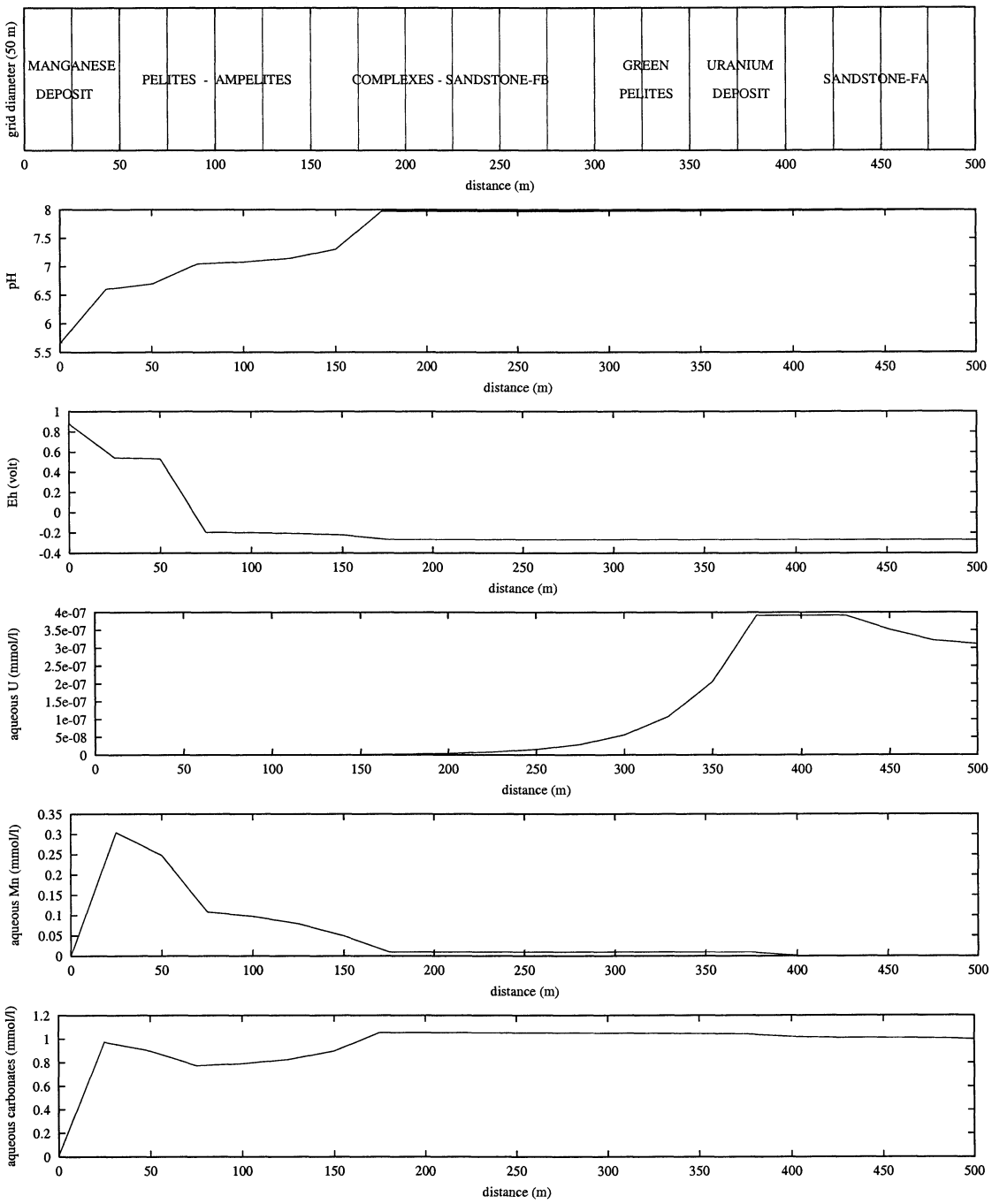

Figure 5-4 HYTEC-1D Modelling (time = 50 years): Evolution of pH and Eh values, aqueous concentrations of U, Mn and HCO_3^- in mmol/l along a flow line.

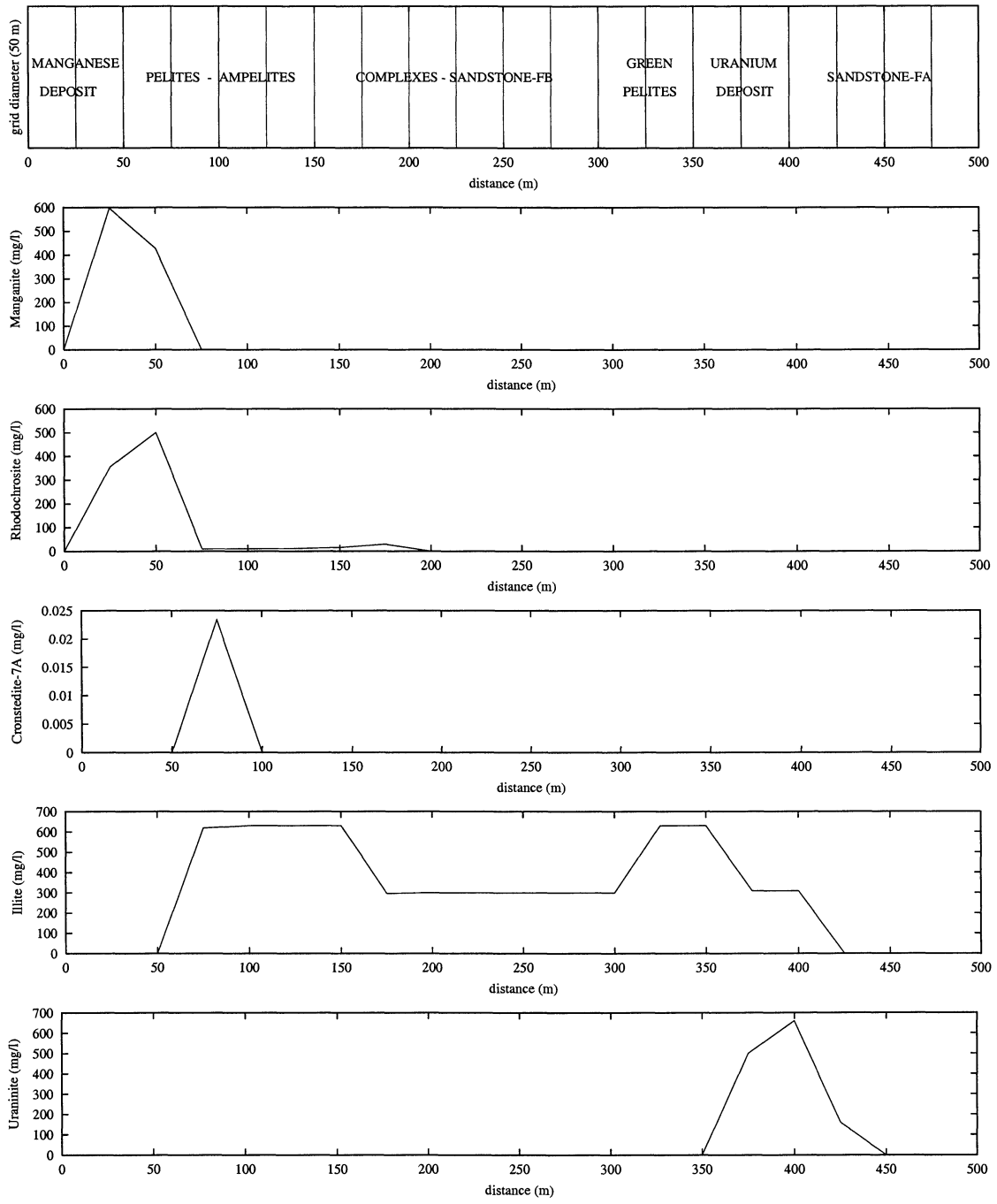

Figure 5-5 HYTEC-1D Modelling (time = 50 years): Evolution of the amount of minerals (Manganite, Rhodochrosite, Cronstedtite, illite, uraninite) in mg/l along a flow line.

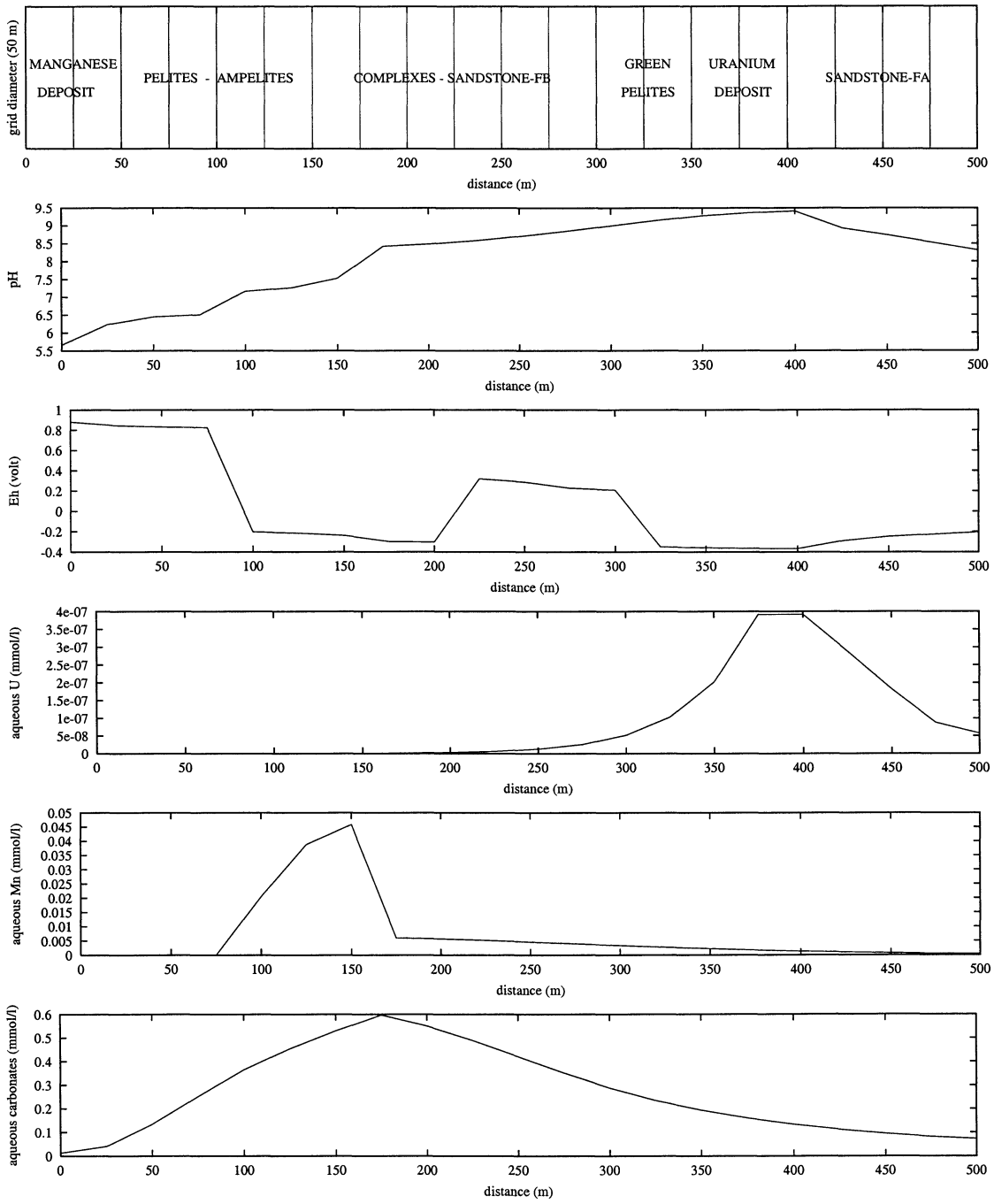

Figure 5-6 HYTEC-1D Modelling (time = 10 years): Evolution of pH and Eh values, aqueous concentrations of U, Mn and HCO_3^- in mmol/l along a flow line.

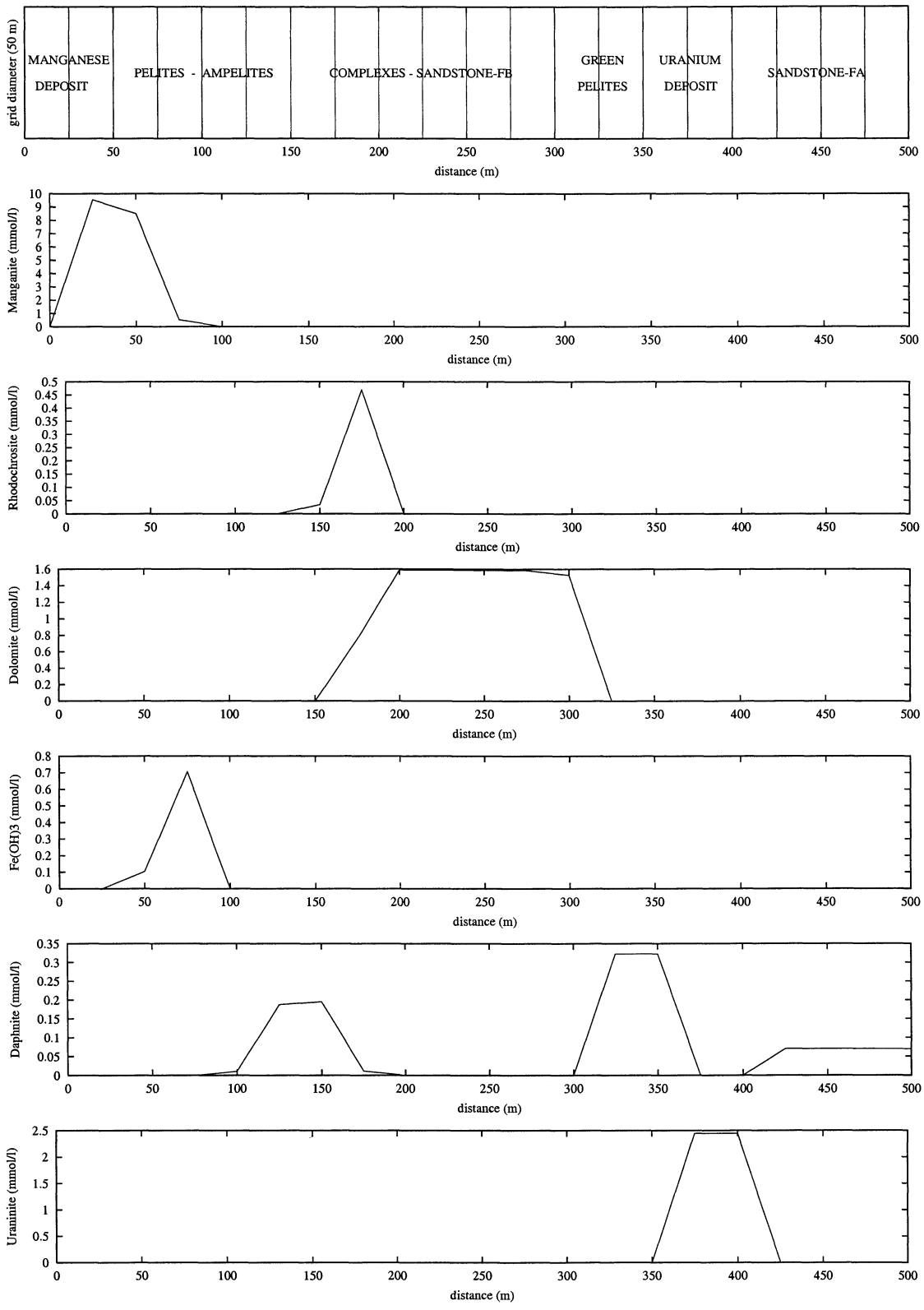

Figure 5-7 HYTEC-1D Modelling (time = 10 years): Evolution of the amount of minerals (Manganite, Rhodochrosite, dolomite, $Fe(OH)_3$, daphnite-14A, uraninite) in mmol/l along a flow line.

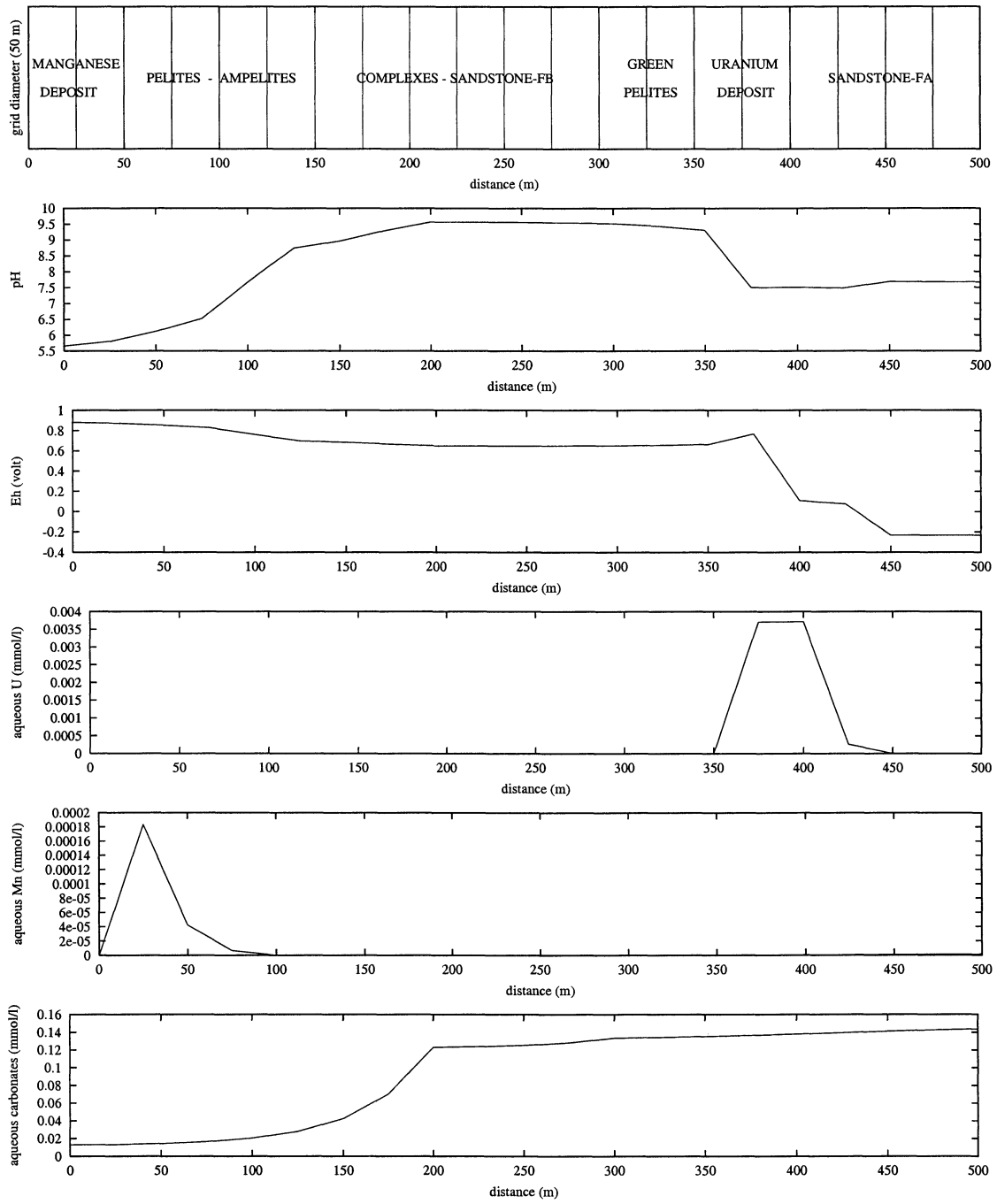

Figure 5-8 HYTEC-1D Modelling (time = 60 years): Evolution of pH and Eh values, aqueous concentrations of U, Mn and HCO_3^- in mmol/l along a flow line.

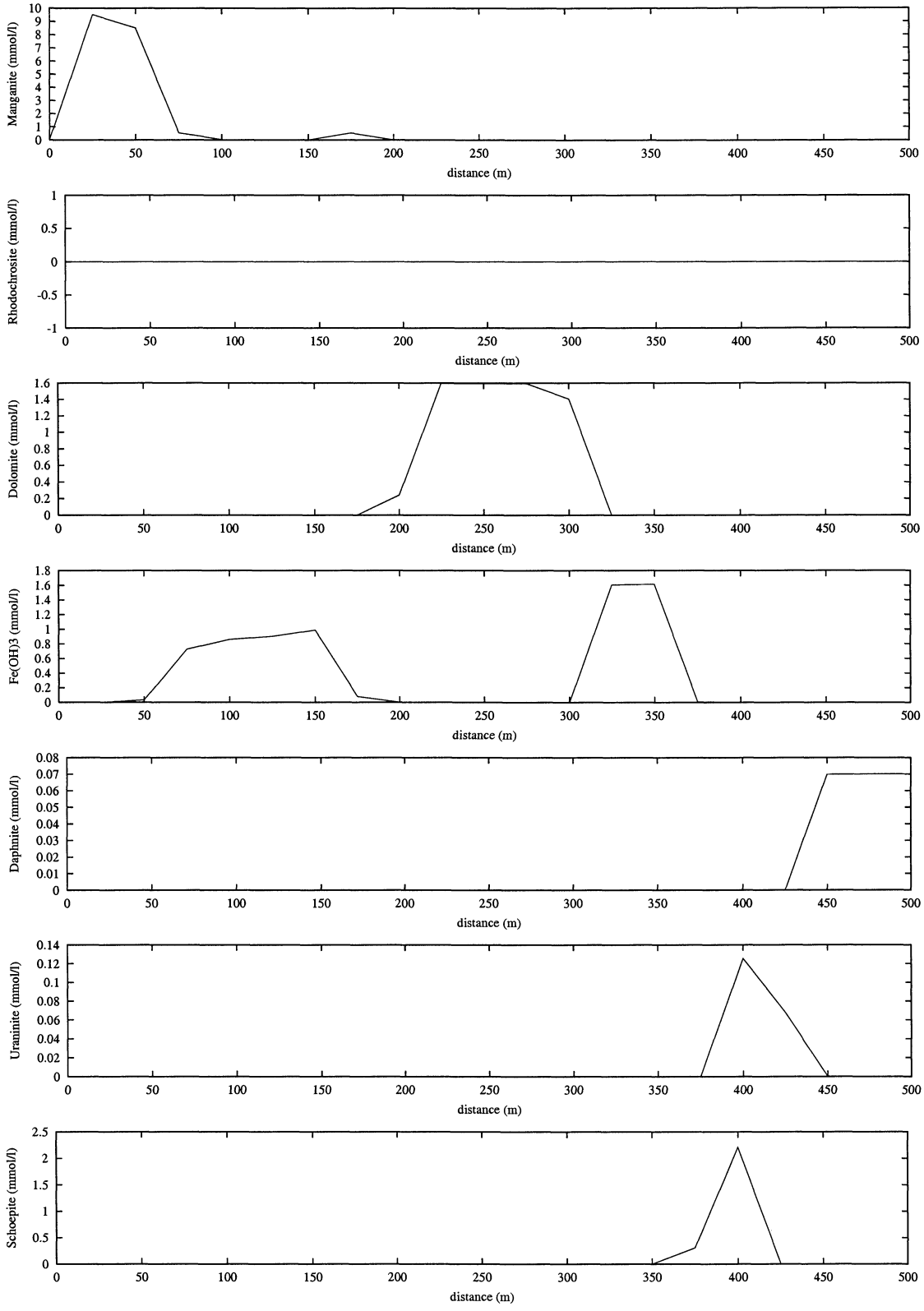

Figure 5-9 HYTEC-1D Modelling (time = 60 years): Evolution of the amount of minerals (Manganite, dolomite, $Fe(OH)_3$, daphnite-14A, uraninite, schoepite) in mmol/l along a flow line.

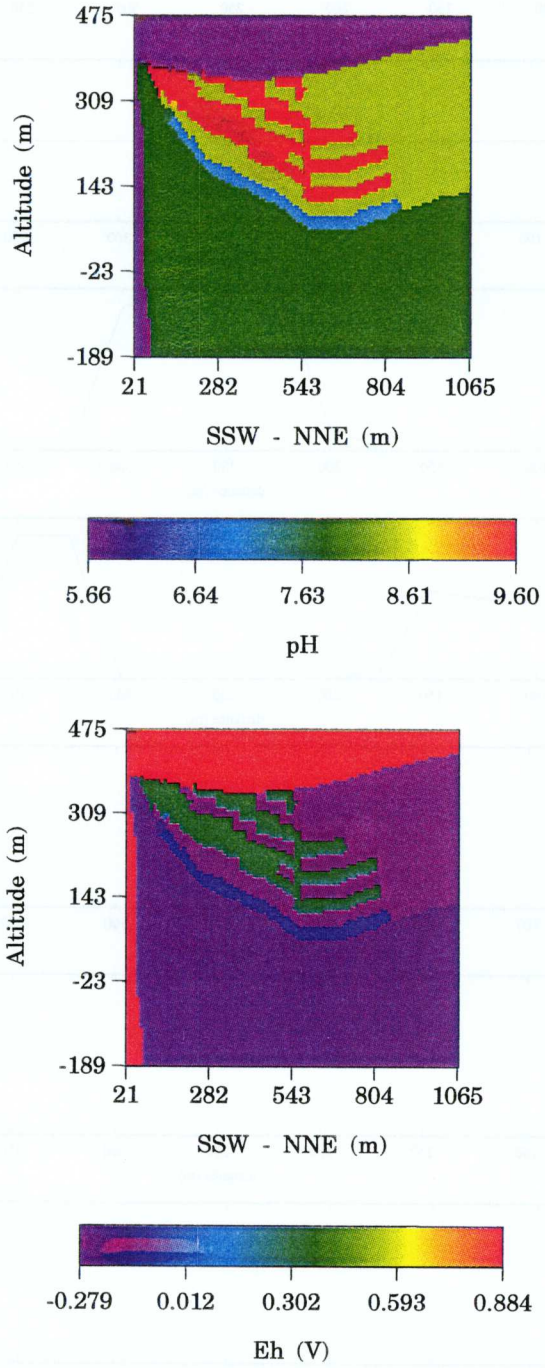

Figure 5-10 HYTEC-2D Modelling: initial conditions of pH and Eh values.

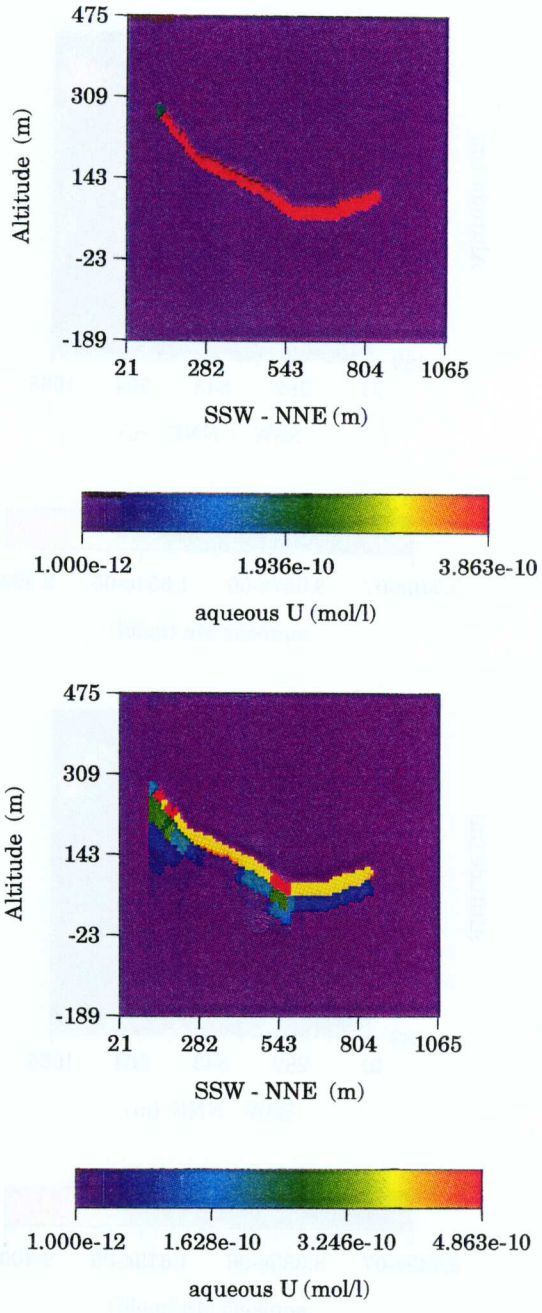

Figure 5-11 HYTEC-2D Modelling: (i) initial condition of aqueous U (mol/l) and (ii) evolution of aqueous U in mol/l after 5 years.

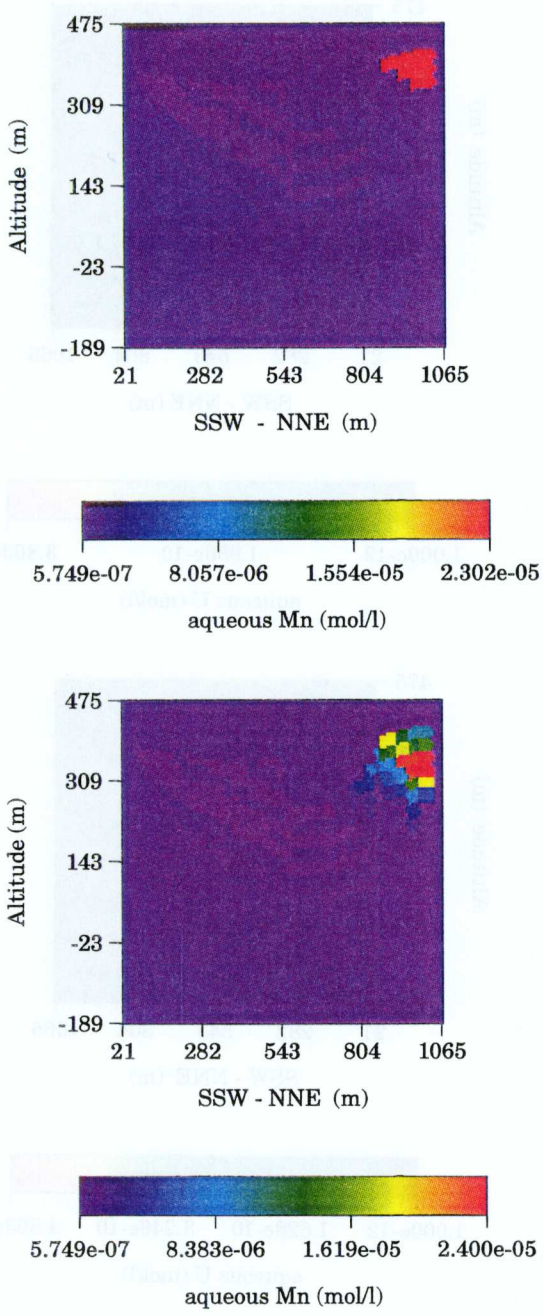

Figure 5-12 HYTEC-2D Modelling: (i) initial condition of aqueous Mn (mol/l) and (ii) evolution of aqueous Mn in mol/l after 5 years.

5.4 RESULTS OF HYTEC-1D MODELLING

Two scenarios have been carried out according to the flow rate of groundwater into the Okélobondo site:

- the first, with a "Darcy velocity" obtained from the hydrodynamic model proposed by Gurban (1996) equal to $2x10^{-10}$ m/s. The modelling results of this option are presented in figures 5-3 (after 4 years), 5-4 and 5-5 (after 50 years).
- the second, with a high "Darcy velocity" equal to $2x10^{-7}$ m/s (main water flux = $3.927x10^{-8}$ m^3/s) corresponding to a rapid flow in the fault system as the example (SSW of the 2D cross section; figure 4-1). The modelling results of this option are explained in figures 5-6, 5-7 (after 10 years) and 5-8, 5-9 (after 60 years).

In figure 5-3, after 4 years, the results of hydro-geochemical HYTEC-1D modelling show a progression of acidic pH in the pelites-ampelites zone until about 175 m. The Eh is buffered around -250 mV in the pelites-ampelites zone by the precipitation of a chlorite type mineral as cronstedtite-7A. After the uranium deposit zone, a slight plume of U is simulated (from $4x10^{-10}$ to $5x10^{-11}$ mol/l). Moreover, a migration of Mn^{2+} is observed below the manganese deposit under the influence of acidic and oxidising rain water. In figure 5-4 (after 50 years), the pH calculated is close to 8 from the complexes zone to the sandstone-FA zone. The Eh is buffered by the equilibrium between illite–chlorite (cronstedtite-7A) or illite - magnetite minerals around -250 mV. A slight migration of aqueous uranium is observed down stream the uranium deposit; the U concentration varying from $4x10^{-10}$ to $3.1x10^{-10}$ mol/l. A plume of Mn^{2+} is simulated below the manganese deposit.

Figure 5-5 shows the relative stability of Manganite under oxidising rain water flow. On the other hand, the rhodochrosite is destroyed and finally controls the Mn^{2+} aqueous concentration at the front and into the complexes/sandstone-FB zone. A small dissolution of uraninite is simulated at the green pelites/uranium deposit interface according to the slight aqueous uranium migration observed in figure 5-4. Behind the mineralised layer, a small amount of uraninite precipitates.

The modelling results with a high "Darcy velocity" (main water flux = $3.927x10^{-8}$ m^3/s) corresponding to a rapid flow in the fault system for example are explained in figures 5-6 to 5-9. In figure 5-6 (after 10 years), an acidic and oxidising groundwater front is observed in the pelites-ampelites zone. A plume of Mn^{2+} aqueous concentration is simulated behind the manganese deposit zone. A precipitation of $Fe(OH)_3$ is correlated with the progress of the rain water type. The manganite is stable under the oxidising water and the rhodochrosite reprecipitates at the interface pelites/complexes where Eh is reduced and aqueous concentration of carbonates sufficient (figure 5-7). In figure 5-7, the equilibrium with respect to daphnite-14A and illite controls the Eh around -250 mV. The uraninite zone remains stable. In figure 5-8 (after 60 years), the influence of the progress of oxidising and acidic groundwater is observed until the uranium deposit zone where the Eh value is close to 700 mV. The manganite remains stable in the geochemical system but the rhodochrosite is entirely destroyed (figure 5-9). No plume of aqueous uranium down stream the mineralised layer is simulated (figure 5-8). The uraninite is dissolved under oxidising groundwater and the aqueous uranium reprecipitates in solid phase U(VI) as schoepite (figure 5-9). The precipitation of $Fe(OH)_3$ is observed in pelites-ampelites and green pelites zones (figure 5-9). Behind the uranium deposit, the reducing Eh is controlled by the daphnite-14A/illite equilibrium.

5.5 RESULTS OF HYTEC-2D MODELLING

In figure 5-11, a plume of aqueous uranium down stream the uranium deposit is simulated. This slight migration can be explained by the influence of oxidising water penetrating in the geochemical system by the fault (SSW, at left of the cross section) or by the pelites and complexes facies (NNE, at right of the cross section). The aqueous concentration of uranium remains at a low value from $4.8x10^{-10}$ mol/l in the uranium deposit to $1.0x10^{-11}$ mol/l below the mineralised layer.

In figure 5-12, an oxidation of the manganese deposit under the rain water flow involves a plume of aqueous Mn^{2+}. The aqueous concentration of manganese varies from $2.4x10^{-5}$ mol/l, controlled by the solid phase Manganite (MnO_2), to $5.0x10^{-7}$ downstream the manganese deposit and controlled by the Rhodochrosite mineral ($MnCO_3$).

These HYTEC-2D results are similar to those obtained along flow lines using the HYTEC-1D code shown above.

6 M3 MODELLING

6.1 METHOD DESCRIPTION

Many variables and different sampling campaigns are important for the understanding of the natural system. The information gathered in many variables can be handled using multivariate techniques.

The origin and evolution of the groundwater can be described if the effect from mixing and reactions can be examined separately. In order to do this separation a new method named Multivariate Mixing and Mass balance calculations (abbreviated to M3) was constructed (Laaksoharju *et al.*, 1995; Laaksoharju and Skårman, 1997). The model consists of 3 steps where the first step is a standard principal component analysis, followed by mixing, and finally by mass balance calculations (see figure 6-1) according to:

1. A standard multivariate technique called Principal Component Analysis (PCA) which is used for the clustering of the data using the major components Cl, Ca, K, Na, Mg, Mn, SO_4 and HCO_3. PCA aims to describe as much of the information from the ten variables in the first equation (called the first principal component) as possible. As much as possible of the remaining information is described by the second principal component. The principal components are equations of linear combinations that describe most of the information in the data. The weights for the different variables in the equations are calculated automatically by the PCA. For the Okélobondo data set the first two principal components can be used to describe 60% of the information in the data set. The third or fourth principal components generally do not contain useful information but this is dependent on the complexity of the examined data and the chosen variables. If the first two principal components contain most of the information, an x, y scatter plot can be drawn. The x is the equation for the first principal component and y the equation for the second principal component. The plot is named the M3 plot and is used to visualise the clustering of the data as well as to identify extreme waters. Extreme waters can be an end-member composition such as rain water, deep water or intermediate water (see figure 6-1). Lines are drawn between the extreme waters so a polygon is formed. The polygon defines the observations, which can be described by the selected extreme waters. By definition the selected extreme waters can describe the observations inside the polygon. The groundwater composition of an observation inside the polygon is compared to the chosen extreme water compositions.

2. Mixing calculations are used to calculate the mixing portions. The mixing portions describe the contribution of the end-member to the observed water. The calculated mixing portion can be used to describe the origin of the groundwater. The mixing portions are equal to the distance to the selected reference waters or end-members in the M3 plot (see figure 6-1). From a two-dimensional surface, mixing portions containing a maximum of three reference waters can be calculated so that a mathematically unique solution is obtained. To avoid this shortcoming and to be able to use more than three reference waters in the model a control point with a known mixing portion was added to the calculations. A polygon containing three reference waters contains a portion of 33.3% of each reference water in the centre point. By using this addition a mathematically unique solution can be achieved from a two dimensional plane with more than three reference waters (Laaksoharju *et al.*, 1998).

A mixing portion calculation of less than 10% is regarded as under the detection limit for the M3 method and is therefore uncertain.

3. Mass balance calculations are used to define the sources and sinks for different elements which deviate from the ideal mixing model used in the mixing calculations. The mixing portions are used to predict new values for the elements. No deviation from the measured value indicates that mixing can explain the element behaviour. A source or sink is due to mass balance reactions. The evolution of the groundwater can thus be described.

The M3 model can describe the origin and evolution of the groundwater chemistry by means of the major mixing processes and mass balance reactions. It is important to note that the modelling is always relative to the selected reference waters or end-members. The modelling constraints can be changed depending on the selection of extreme waters. It is important to note that the M3 model deals only with chemical information; no space or time constraints are included in the model.

Back-propagation test mixtures of groundwaters were modelled using the M3 concept and show that the accuracy of the mixing calculations is generally ±10.5% (Laaksoharju and Wallin (Eds.), 1997). Small errors in the prediction of conservative element behaviour may lead to large errors in the mass balance calculations. A low resolution may lead to difficulties in identifying the end-members and in correctly modelling the system.

6.2 MODELLED AREA

The CD cross-section (figure 4-1) is used to support the M3modelling. The minimum and maximum x,y,z of the model are:

X min= 295565 (OK2) X max= 296240 (SA992)

Y min= 9842625 (SA992) Y max= 9843078 (SA31)

Z min= -34 (SA997) Z max= 440 (surface)

6.3 SELECTION OF THE END-MEMBERS FOR THE M3 MODELLING

The PCA plot in M3 is a useful tool to identify the end-members in relation to the hydrodynamic model made by Gurban *et al.* (figure 6-1).

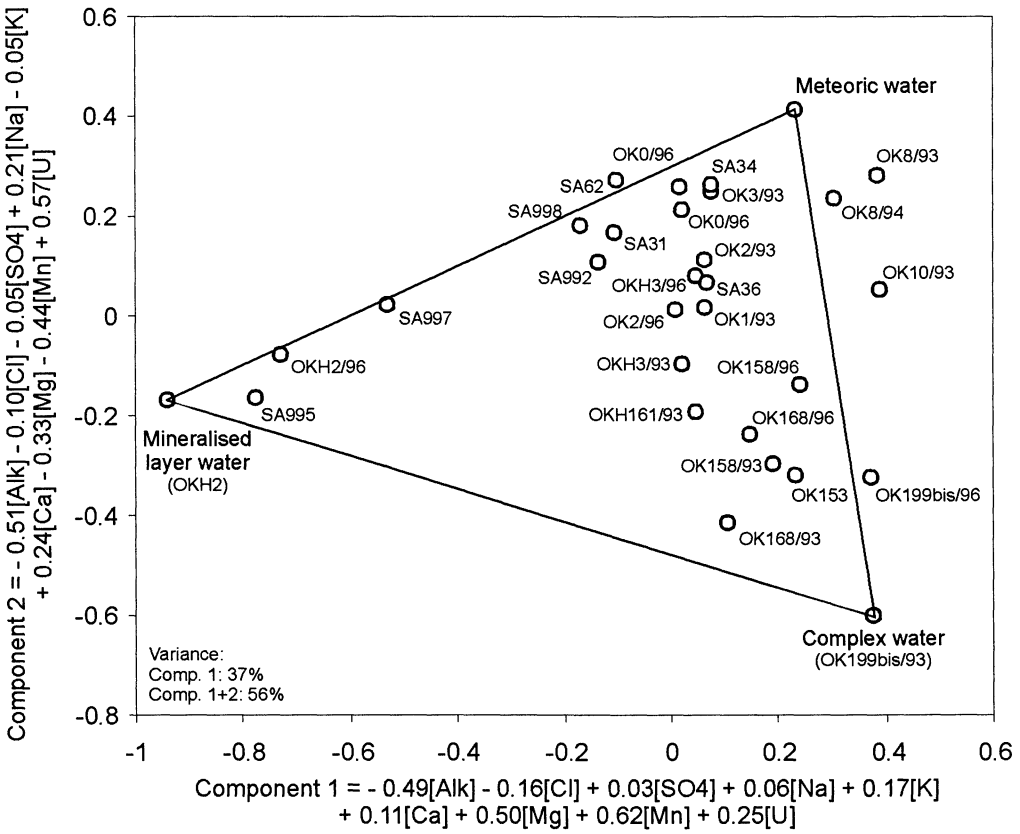

Figure 6-1 PCA plot, identification of the samples and end-members.

The selected end-members for the current modelling are shown in figure 6-1 in relation to the sampled groundwaters at Okélobondo. The ID codes for the chosen reference waters are shown. The end-members were selected so that most of the samples can be described. The criteria are by definition that a sample inside the polygon can be described by the selected end-members. The closer to the end-member a groundwater observation plots in PCA the more of that end-member the water contains. The reason for modelling all the campaigns simultaneously by using the same end-members is that the maximum amount of information about the whole system can be obtained at the same time and the evolution of the geochemistry can be compared.

The analytical data for the end-members are listed in Appendix 1. The selected end-members for M3 Okélobondo modelling are:

- **Meteoric: corresponding to the precipitation and infiltration water (row 30 in Appendix 2)**

- **Mineralised layer water: described by OKH2an, water found in OKH2an and from the U mineralisation (row 5 in Appendix 2)**

- **Complexes water: described by OK199bis, water in complexes formation, characterised by the ratio Ca/Mg = 1 (row 14 in Appendix 2).**

6.4 3D VISUALISATION OF THE M3 CALCULATIONS

In order to visualise the distribution of uranium, alkalinity, calcium, sulphate, magnesium, manganese and chloride and the results of the mixing portion calculations of rain, mineralised layer water and complexes water, a 3D interpolation was performed using Voxel Analyst by INTERGRAPH.

The vertical cross-section from OK2 to SA992 was selected to show the distribution of the salinity and dominating water types, alkalinity, Ca, SO_4, Mg, uranium and Mn, and this also reflects the specific geological structures. The geological structures are from top to bottom: pelites 3, ampelites, complexes 2, sandstones GF1b, pelites 2, complexes 1, pelites 1 and green pelites. The boreholes are shown in figures 4-1 and 6-2 to 6-9.

The modelling is based solely on chemical information which can be used to support the 3D understanding of groundwater flow through the site area. The calculated mixing portions are always relative to the selected reference water. The distribution of the chosen major elements, salinity and uranium in portions of rain, deep and intermediate water are shown in figures 6-2 to 6-9.

The cross-sections show the measured values on the left side and the deviation calculated with M3 from the measured values on the right side. The deviations can be positive or negative, showing a gain or a loss in the system, due to reactions or biological processes.

The results of the mixing calculations for all observations are listed in Appendix 1.

6.4.1 Visualisation of M3 modelling

The M3 modelling results are presented in the following figures (figures 6-2 to 6-9). A comparison of the U deviation plot and the Mn deviation plot showed an almost mirror behaviour. The U transport stops when the Mn gain increases.

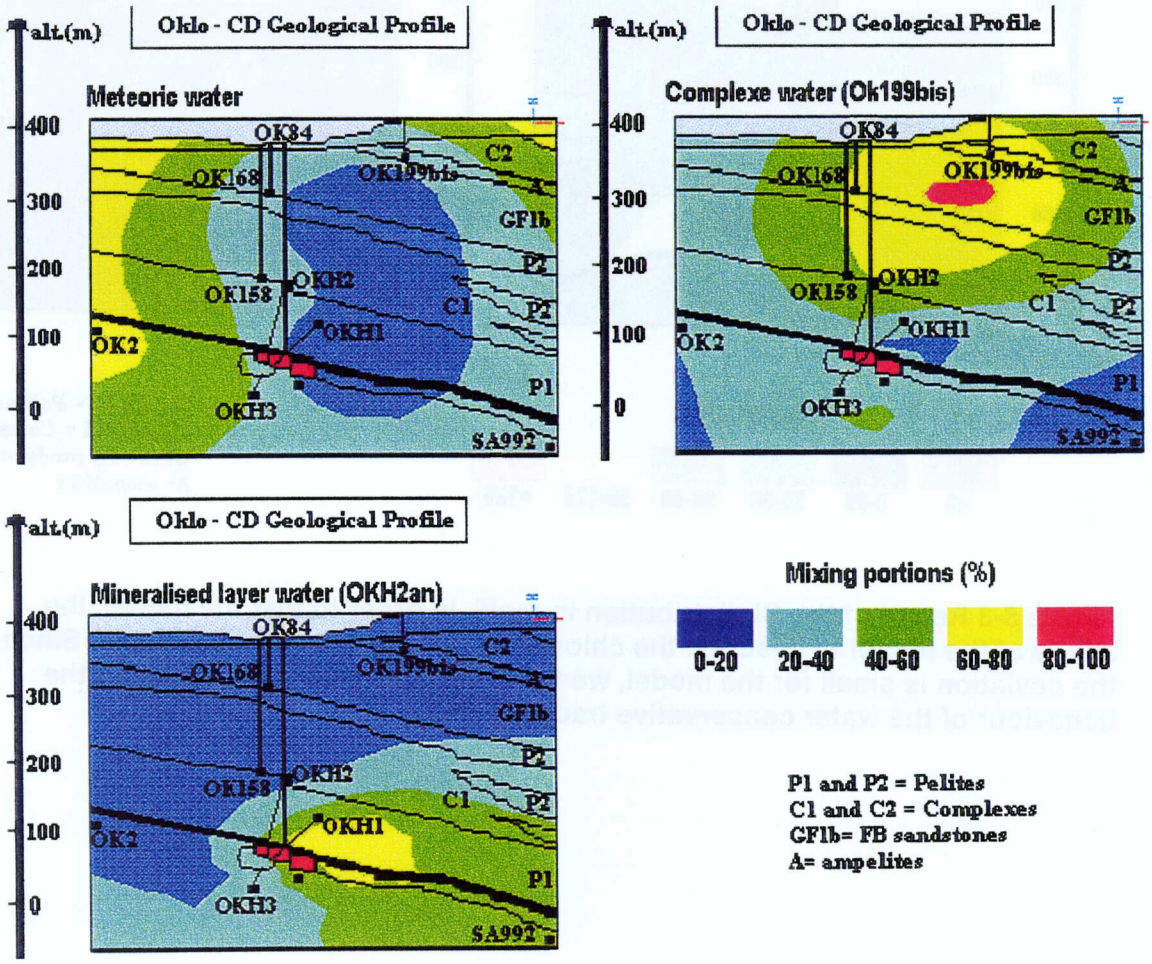

Figure 6-2 Result of the M3 modelling of the rain, complexes water and mineralised layer (%). The rain, coming from the sides in the domain is in good agreement with the hydrodynamic model. The deep water is present in a very small proportion at the surface, increasing towards the bottom where it is 100%. A high proportion of complexes water is present in the complex formation.

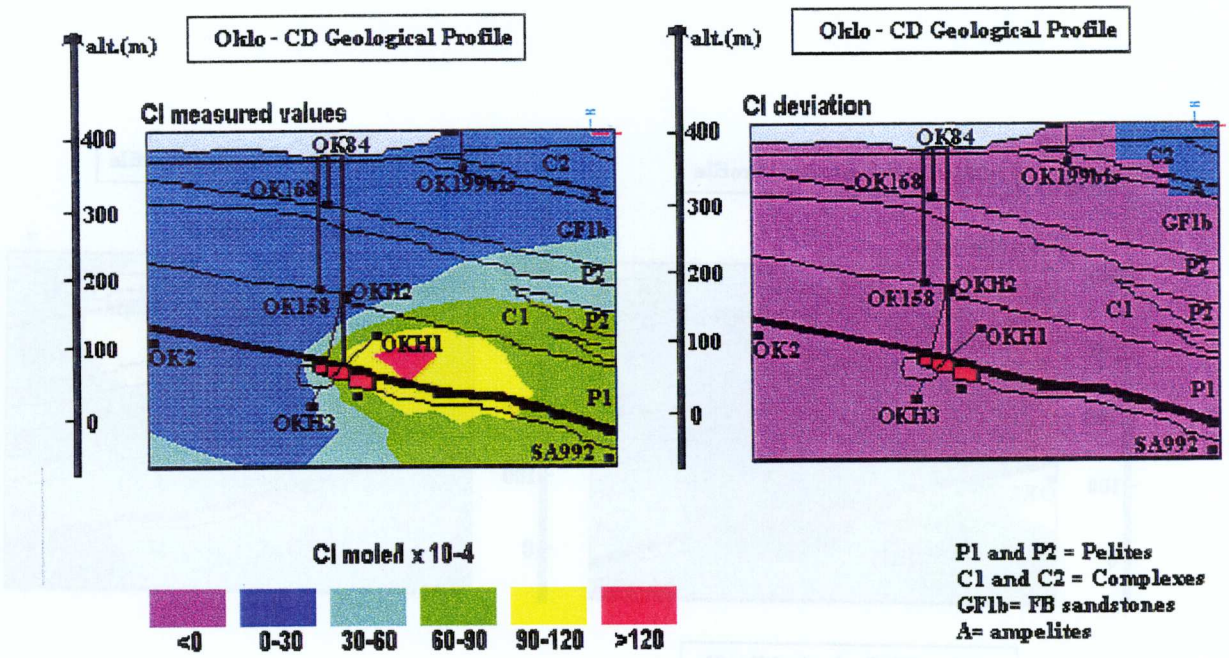

Figure 6-3 Result of the Cl distribution in mol/l. In order to test the model, the ability of the model to describe the chloride distribution was investigated. Since the deviation is small for the model, we think that the model can describe the behaviour of the water conservative tracer Cl well.

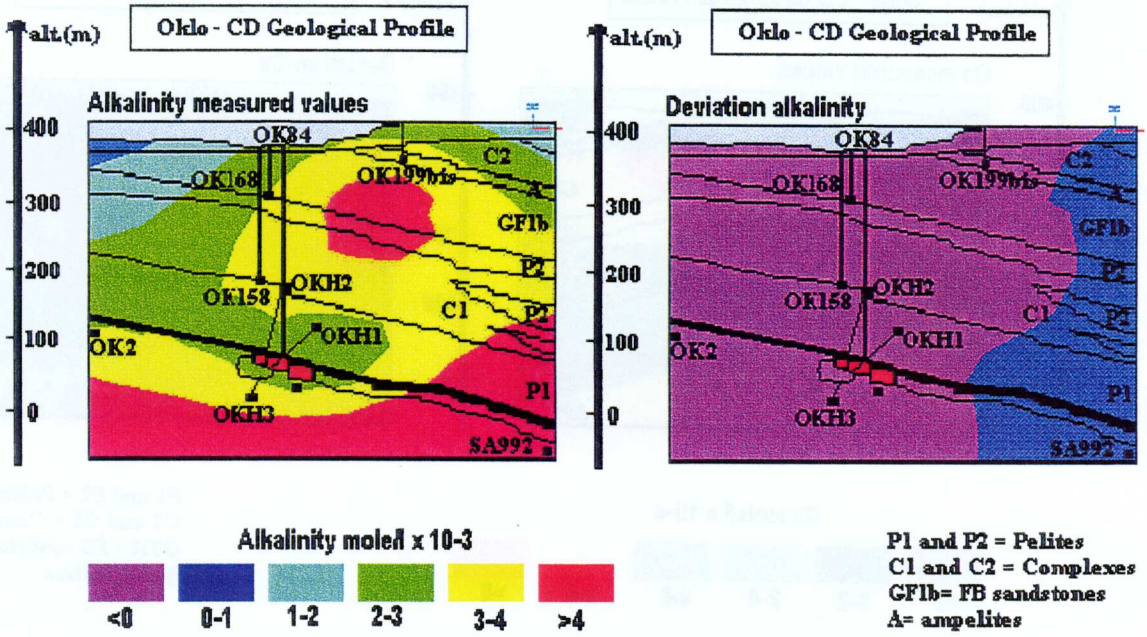

Figure 6-4 Result of the alkalinity distribution in mol/l. The left picture shows the measured values, the right picture the modelled values with M3. High values of alkalinity are observed in the complexes and mineralised layer waters. The deviation plot shows a gain in the right corner of the model, associated perhaps with the influx of meteoric water. In the rest of the domain a loss of alkalinity in comparison with the measured values is observed.

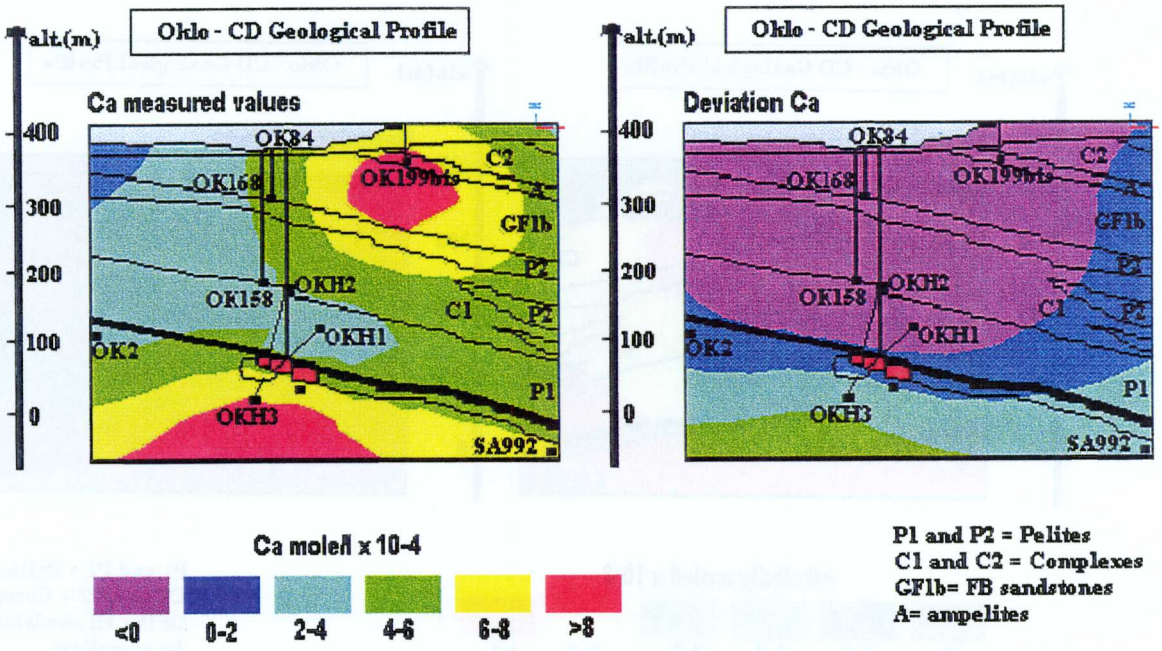

Figure 6-5 Result of the Ca distribution in mol/l. The left picture shows the measured values, the right picture the modelled values with M3. High values of Ca in the complexes formation and below the reactor are observed. A gain of Ca is shown in the right part of the deviation plot, which can then indicate a possible dissolution of calcite, in good agreement with the alkalinity increase in figure 6-4. It is thus possible that an inorganic reaction is dominating this part of the system.

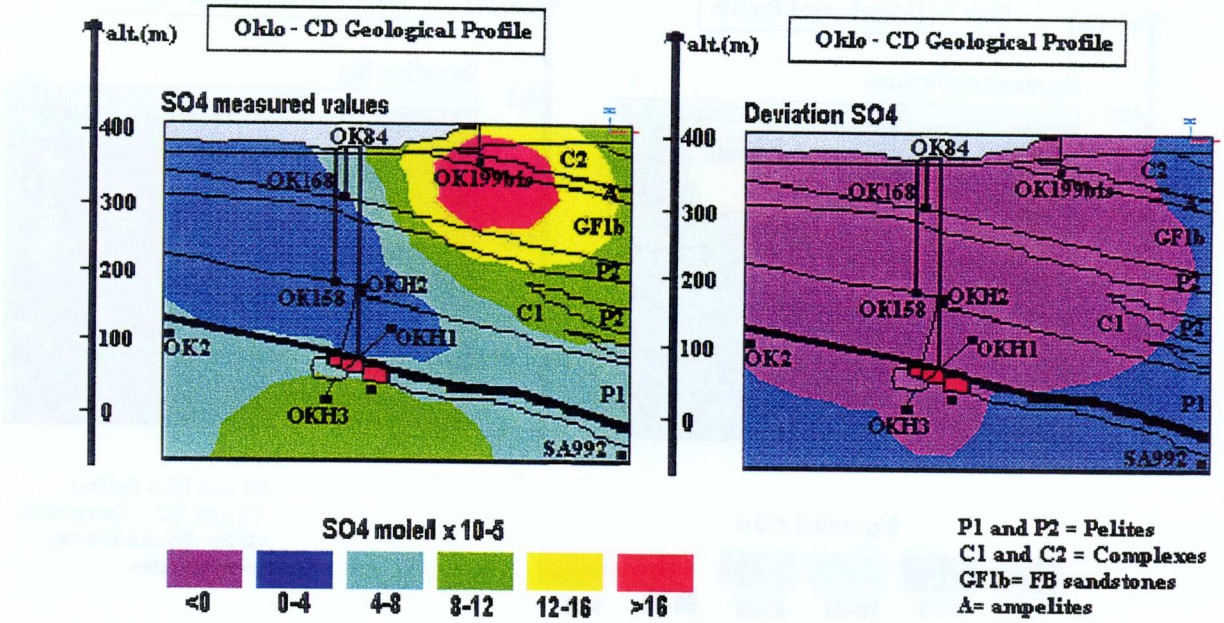

Figure 6-6 Result of the SO_4 distribution in mol/l. The left picture shows the measured values, the right picture the modelled values with M3. SO_4 can be used as an indicator of pyrite oxidation. In the left picture high values in the complexes formation and increased values below the reactor are observed. The M3 deviation plot shows a gain of sulphate in the right part and in the lower left part of the model, which can be associated with oxidation of pyrite made by inflowing meteoric water.

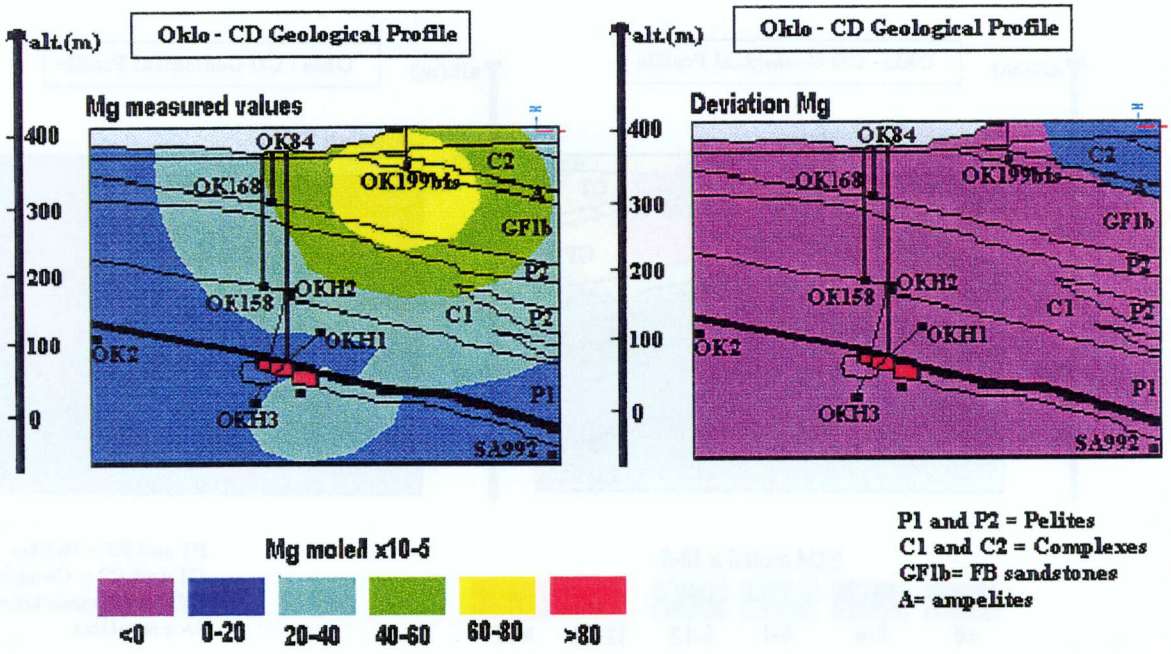

Figure 6-7 Result of the Mg distribution in mol/l. The left picture shows the measured values, the right picture the modelled values with M3. The measured high Mg values indicate groundwater in contact with Mg rich minerals. In the left picture high measured values associated with the complexes formation are observed. The M3 deviation shows a gain of Mg in the right upper corner, associated perhaps with Mg dissolution.

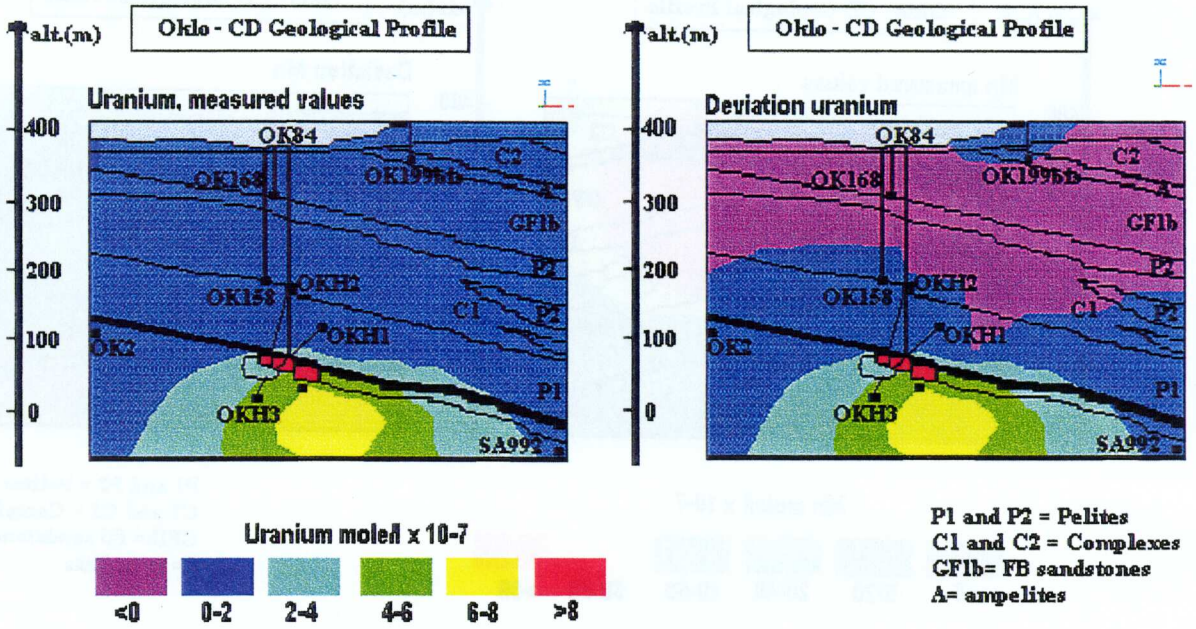

Figure 6-8 Result of the U distribution in mol/l. The left picture shows the measured values, the right picture the modelled values with M3. The U measured values show increased values of U in the mineralised layer. The M3 U deviation plot shows an increase of U around the mineralised layer which can be a result of oxidation of U minerals. However, the model shows that it is not a direct U transport towards the surface.

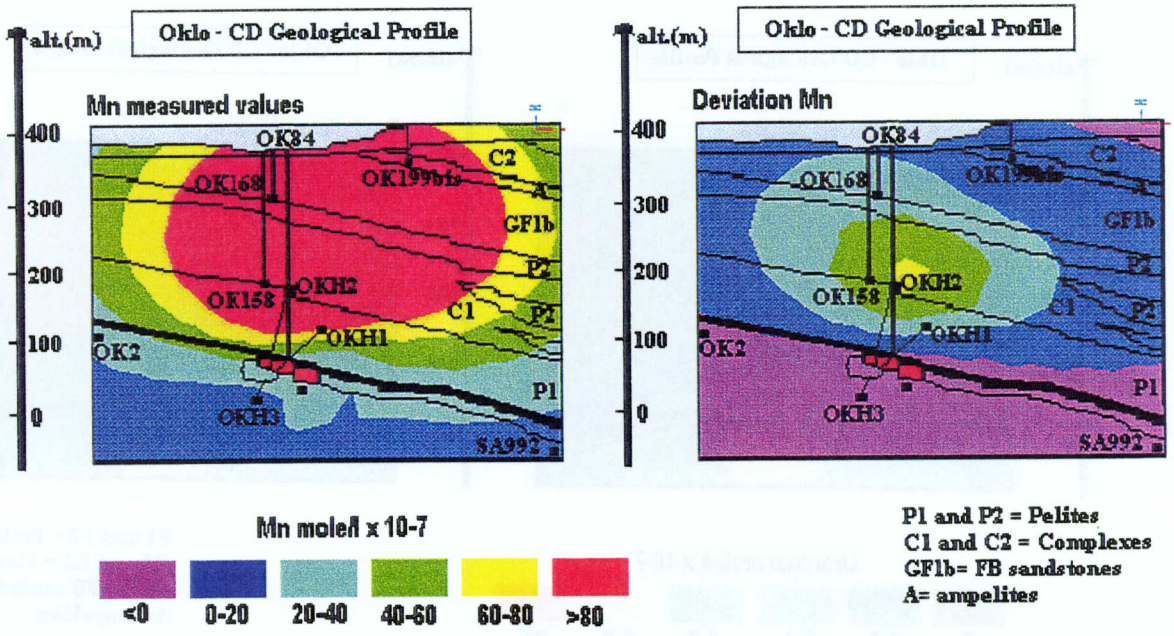

Figure 6-9 Result of the Mn distribution in mol/l. The left picture shows the measured values, the right picture the modelled values with M3. The left picture shows high measured values of the Mn associated with the FB formations (complexes, sandstones F1b and pelites). The M3 deviation for the Mn shows a gain of Mn which can indicate oxidation of Mn minerals. According to the hydrodynamic model, this oxidation is generated by the recharge waters coming into the system through the more permeable complexes units or by the upward waters coming from the depth and which were in contact with the mineralised layer. The Mn oxidation may consume the oxygen and hinder U transport up to the surface, acting as an inorganic trap.

6.5 M3 MODELLING RESULTS

M3 shows that inorganic reactions are dominating the system.

The measured values of U (uranium) (figure 6-8) show increased values in the mineralised layer. The M3 deviation plot of U shows an increase of U around the mineralised layer which can be a result of oxidation of U minerals. However, the model shows that it is not a direct U transport towards the surface.

The M3 deviation for Mn (manganese) (figure 6-9) shows a gain which can indicate oxidation of Mn minerals. According to the hydrodynamic model, this oxidation is generated by the recharge waters coming into the system through the "complexes units" which are more permeable or by the upward flowing waters coming from the depth and which were in contact with the mineralised layer. The Mn oxidation may consume the oxygen and hinder U transport up to the surface, acting as an inorganic trap. The reason for not having U transport up to the surface in Okélobondo is believed to be due to inorganic Mn oxidation that probably makes the water less oxidising and the U transport more difficult. The other possibility is a stronger influx of water from the sides which dilutes the effects from the uranium transport.

A comparison of the U deviation plot and the Mn deviation plot showed an almost mirror behaviour. The U transport stops when the Mn gain increases.

7 CONCLUSIONS

During the previous exercise at Bangombé, it was realised that the codes complement each other and a better understanding of the geochemical studied system is thus obtained (Gurban *et al.* 1998). The same procedure is now applied to the Okélobondo site. First the M3 modelling was completed. M3 can relatively easily be used to calculate mixing portions and to identify the sinks or the sources that may exist in a geochemical system. This can help to address the reactions in the coupled code such as HYTEC-1D/2D, to identify the system and to reduce the computation time.

M3 and HYTEC (-1D, -2D) models, both show a gain of alkalinity in the whole modelled area.

M3 shows a dissolution of the uranium layer in contact with upwardly oxidising waters. The HYTEC-1D modelling shows (figure 5-5) a small dissolution of uraninite at the green pelites/uranium deposit interface according to the slight aqueous uranium migration observed in figure 5-4 This plume of aqueous uranium down stream the uranium deposit can be explained by the influence of oxidising water penetrating in the geochemical system by the fault (SSW, at left of the cross section) or by the pelites and complexes facies (NNE, at right of the cross section).

M3 shows an gain of manganese rich minerals downstream the reactor. HYTEC shows that the rhodochrosite is destroyed and finally controls the Mn^{2+} aqueous concentration at the front and into the complexes/sandstone-FB zone. A plume of Mn^{2+} aqueous concentration is simulated behind the manganese deposit zone.

A comparison of the U and Mn plots for M3 deviation and HYTEC results showed an almost mirror behaviour. The U transport stops when the Mn gain increases.

The reactive transport results (one dimensional and two dimensional simulations) are in good agreement with the statistical approach using the M3 model. Thus, HYTEC and M3 modelling predict that a possible reason for not having U transport up to the surface in Okélobondo is due to an inorganic trap which may hinder the uranium transport.

By using an inter-comparison of the two independent modelling approaches, we can better understand the processes that can take place in nature. Thus, we can build confident tools which can be used for long term predictions of performance assessment of a site.

8 FUTURE WORK

Due to the results of this exercise, during the Oklo 2nd Phase meeting, held in Cadarache on the 20th and the 21st of May 1999, the importance and usefulness of applying different approaches to explain a hydro-geochemical system was presented. This provides the opportunity to assess the necessary tools for future performance assessment of the prospective real waste repository sites.

ACKNOWLEDGEMENTS

This study has been supported and financed by the Swedish Nuclear and Waste Management Company (SKB) and ARMINES, France. The helpful discussions from Fred Karlsson (SKB), John Smellie (Conterra AB) are acknowledged. Cecilia Andersson (INTERA KB) helped with finalising the document. Izabella Halberg (Hallberg Translations) corrected the language.

REFERENCES

Bruno J., Duro L. and Arcos D. (1997) - Blind Prediction Modelling Exercice in Oklo.2nd stage : Uranium in Okélobondo. Report QuantiSci, Spain.

Cordier, E. and Goblet, P. (1996) Programme MÉTIS: Simulation d'écoulement et de transport miscible en milieu poreux et fracturé. Version 2.0. Notice d'emploi, CIG/EMP - LHM/RD/96/08.

Dewindt L. and van der Lee J. (1999) -Cahier d'application du code couplé chimie-transport HYTEC-1D, version 2.4. Report Ecole des Mines de Paris - CIG, LHM/ RD/99/17.

Goblet, P. (1981), Modélisation des transferts de masse et d'énergie en aquifère, 1981, Ecole Nationale Supérieure des Mines de Paris - Université Pierre et Marie Curie.

Gurban, I. (1996) Caractérisation et modélisation de l`écoulement et du transport de matière au voisinage des réacteurs nucléaires naturels d`Oklo, Gabon, *Thése de doctorat, Ecoles des Mines de Paris*, Mémoires des Sciences de la Terre, Nr. 25, 194p.

Gurban I, Laaksoharju M., Ledoux E. and Madé B., Salignac, AL (1999) - Indications of uranium transport around the reactor zone at Bangombé (Oklo). SKB Technical Report 98-06, Stockholm, Sweden.

Gurban I, Ledoux E, Made B, Salignac A-L, Winberg A, Smellie J, Louvat D, Toulhoat P, (1996). Oklo, analogue naturel de stockage de déchets radioactifs (phase 1). Volume 3. Caractérisation et modélisation des migrations à distance des zones de réaction (sites d'Okélobondo et de Bangombé), Nuclear Science and Technology, Commision of the European Communities, Rapport Final.EUR Rep. 16857/3 FR, 177p.

Laaksoharju M, Skårman C, Skårman E, 1998. Multivariate Mixing and Mass balance (M3) calculations, a new tool for decoding hydrogeochemical information. Submitted to Applied Geochemistry.

Laaksoharju M, Wallin B (eds), 1997. Evolution of the groundwater chemistry at the Swedish Äspö Hardrock Laboratory site. Proceedings of the second Äspö international geochemistry workshop. SKB International Cooperation Report 97-04, Stockholm, Sweden.

Madé B. et Salignac A.L. (1998) Modelisation couplee chimie-transport de la zone de reaction sur le site de Bangombé (Oklo, Gabon). LHM/RD/98/4.

Madé B. and Ledoux E. (1999) - Coupled chemical transport modelling at Okélonbodo site (Oklo-natural analogue, Gabon). Report Ecole des Mines de Paris - CIG}, LHM/ RD/99/19.

Madé B., Ledoux E., Ayora C. and Salas J. (1998) Coupled Chemical Transport Modellingof Uranium at Bangombé (Oklo, Gabon). Proceeding of the workshopon Oklo-natural analogue, phase II, june 1998, Helsinki, Finland.

Salas J., Ayora C., Madé B. and Ledoux E. (1998) - Oxidation Processes at Okélobondo Uranium Deposit: Preliminary Reactive Transport Model. Proceeding of the workshopon Oklo-natural analogue, phase II, june 1998, Helsinki, Finland.

Salignac, A.L. (1997) Programme STELE 2: Rapport final, Notice conceptuelle et d'utilisation du modèle HYTEC-2D, CIG/EMP - LHM/RD/97/12.

Toulhoat, P., Gallien, J.P., Louvat, D., Moulin, V., L'Henoret, P., Guerin, R., Ledoux, E., Gurban, I., Smellie, J.A., Winberg, A., (1994) Preliminary studies of groundwater flow and migration of uranium isotopes around the Oklo natural reactors. Fourth Inter. Conf. on the Chemistry and Migration behaviour of Actinides and Fission Products, Charleston, USA, p. 383-390.

van der Lee, J (1997) - HYTEC-1D, un modèle couplé hydro-géochimique de migration de polluants et de colloïdes. Report Ecole des Mines de Paris - CIG}, LHM/RD/97/02.

van der Lee, J (1999) - CHESS, another geochemical equilibrium computer code. Report Ecole des Mines de Paris - CIG, LHM/RD/99/05.

APPENDIX 1: DATA USED

Table 1: List of data used for the present modelling including the chemical composition and the calculated mixing portions.

	Rèf. échantillon	date prélèv.	Alk mole/l.	Cl mole/l.	SO4 mole/l.	Na mole/l.	K mole/l.	Ca mole/l.	Mg mole/l.	Mn mole/l	U mole/l.	Alk Deviation	Cl Deviation
1	OK0	Mar-93	4.28E-03	8.46E-04	8.85E-05	4.83E-03	7.93E-05	1.57E-04	1.23E-05	4.00E-07	1.22E-08	1.61E-03	-2.48E-03
2	OK1	Mar-93	3.37E-03	3.10E-04	9.47E-05	2.00E-03	1.20E-04	7.24E-04	8.64E-05	8.74E-07	4.20E-07	-4.29E-04	-2.82E-03
3	OK2	Mar-93	3.99E-03	5.64E-05	1.67E-04	3.13E-03	9.46E-05	6.49E-04	4.94E-05	1.13E-06	1.05E-08	7.76E-04	-2.91E-03
4	OK3	Mar-93	3.95E-03	2.00E-04	1.67E-04	3.74E-03	6.91E-05	2.74E-04	2.88E-05	5.82E-07	3.78E-09	1.71E-03	-2.29E-03
5	OKH2An	Mar-93	1.28E-02	1.75E-02	6.25E-06	2.98E-02	3.07E-04	1.90E-04	7.82E-05	9.65E-07	1.97E-08	0	0
6	OKH3	Mar-93	3.24E-03	1.10E-03	4.58E-05	1.74E-03	1.41E-04	1.05E-03	8.64E-05	2.31E-06	1.76E-07	-1.62E-03	-2.84E-03
7	OK8	Mar-93	1.43E-04	1.10E-04	5.10E-04	5.65E-04	6.39E-05	2.25E-04	8.23E-05	5.53E-06	3.15E-09		
8	OK10	Mar-93	2.75E-04	6.21E-05	1.67E-04	1.30E-04	7.67E-05	9.48E-05	1.03E-04	1.67E-05	1.34E-08		
9	OK8	Jul-94	1.38E-04	1.25E-04	2.17E-04	1.32E-04	5.44E-05	2.12E-04	1.10E-04	4.36E-06	3.36E-10		
10	OK161	Mar-93	4.99E-03	8.74E-06	1.56E-05	2.26E-03	1.66E-04	5.49E-04	5.35E-04	1.62E-06	1.68E-08	-2.75E-04	-3.77E-03
11	OK153	Mar-93	3.50E-03	7.33E-05	1.56E-04	7.83E-04	8.44E-05	1.02E-03	4.94E-04	4.75E-06	1.23E-06	-1.12E-03	-1.39E-03
12	OK158	Mar-93	3.72E-03	5.36E-05	1.08E-05	1.65E-03	1.79E-04	3.99E-04	3.41E-04	1.69E-05	5.67E-09	-1.07E-03	-1.93E-03
13	OK168	Mar-93	3.48E-03	6.21E-05	1.06E-05	1.13E-03	3.07E-04	4.99E-04	4.03E-04	1.39E-05	6.30E-09	-2.73E-03	-3.36E-03
14	OK199bis	Mar-93	5.28E-03	1.75E-05	2.81E-04	1.04E-03	4.09E-05	1.17E-03	1.03E-03	1.41E-05	1.09E-08	0	0
15	OK158	Sep-96	3.21E-03	3.89E-05	1.04E-06	1.75E-03	4.90E-05	4.54E-04	4.07E-04	1.13E-05	4.20E-09	-1.89E-04	-9.29E-04
16	OK168	Sep-96	3.54E-03	4.98E-05	3.75E-06	1.59E-03	1.55E-04	5.47E-04	4.54E-04	8.40E-06	1.51E-08	-1.21E-03	-2.42E-03
17	OK199bis	Sep-96	2.97E-03	1.97E-05	1.11E-05	2.22E-04	1.54E-05	6.25E-04	5.90E-04	1.77E-05	2.23E-08		
18	OK0	Sep-96	4.45E-03	4.73E-04	5.58E-05	5.11E-03	6.38E-05	2.23E-04	9.57E-05	9.00E-08	6.70E-09	1.57E-03	-2.83E-03
19	OK2	Sep-96	3.75E-03	5.50E-05	7.03E-05	2.05E-03	1.37E-04	9.09E-04	2.50E-07	1.20E-06	3.28E-08	-5.17E-04	-3.85E-03
20	OKH2	Sep-96	1.07E-02	1.31E-02	1.04E-06	2.90E-02	1.72E-04	4.95E-04	6.36E-05	3.70E-07	1.26E-08	1.36E-04	-1.27E-03
21	OKH3	Sep-96	3.17E-03	7.89E-04	1.04E-04	2.08E-03	1.50E-04	4.59E-04	1.21E-05	8.20E-07	6.43E-07	-3.66E-04	-2.44E-03
22	SA31	Sep-96	7.80E-03	1.09E-04	1.64E-04	8.39E-03	7.16E-05	5.03E-04	2.50E-07	5.00E-08	1.76E-08	3.61E-03	-5.09E-03
23	SA32	Sep-96	7.62E-03	1.24E-04	4.01E-05	8.51E-03	3.05E-05	1.56E-04	2.50E-07	2.00E-08	2.50E-09		
24	SA34	Sep-96	3.92E-03	8.10E-05	5.90E-05	4.27E-03	4.81E-05	7.61E-05	1.18E-04	2.00E-08	2.31E-08	1.75E-03	-2.40E-03
25	SA36	Sep-96	2.95E-03	7.71E-05	7.43E-05	1.22E-03	1.02E-04	8.40E-04	2.50E-07	1.30E-06	4.50E-08	-5.10E-04	-2.90E-03
26	SA992	Sep-96	4.95E-03	5.19E-03	9.23E-05	1.13E-02	5.47E-05	5.74E-04	2.50E-07	2.30E-07	6.51E-07	1.60E-04	-5.33E-04
27	SA995	Sep-96	8.85E-03	1.81E-02	1.60E-04	3.47E-02	1.01E-04	1.31E-03	2.50E-07	2.90E-07	3.99E-08	-2.63E-03	2.91E-03
28	SA996	Sep-96	5.23E-03	5.01E-03	2.23E-05	1.15E-02	4.60E-05	4.33E-04	2.50E-07	2.10E-07	3.74E-08	6.49E-04	-1.03E-03
29	SA997	Sep-96	8.96E-03	1.04E-02	7.21E-05	2.34E-02	1.06E-04	6.35E-04	2.50E-07	1.80E-07	5.46E-08	5.70E-04	-9.74E-04
30	pluie		1.33E-05	1.00E-12	1.00E-12	1.00E-12	1.00E-12	1.00E-12	1.00E-12	1.00E-12	1.00E-12	0	0

	Rèf. échantillon	date prélèv.	SO4 Deviation	Na Deviation	K Deviation	Ca Deviation	Mg Deviation	Mn Deviation	U Deviation	Mixing portions from M3 OKH2An	OK199bis	pluie
1	OK0	Mar-93	7.53E-05	-8.72E-04	1.93E-05	7.11E-05	-4.65E-05	-3.84E-07	7.99E-09	19%	4%	77%
2	OK1	Mar-93	1.35E-05	-3.62E-03	5.35E-05	3.56E-04	-2.21E-04	-3.32E-06	4.13E-07	18%	29%	54%
3	OK2	Mar-93	1.11E-04	-2.12E-03	3.46E-05	3.87E-04	-1.67E-04	-1.81E-06	5.02E-09	17%	20%	63%
4	OK3	Mar-93	1.44E-04	-5.80E-04	2.22E-05	1.56E-04	-6.24E-05	-6.52E-07	1.29E-10	14%	8%	78%
5	OKH2An	Mar-93	0	0	0	0	0	0	0	100%	0%	0%
6	OKH3	Mar-93	-6.07E-05	-5.35E-03	5.67E-05	5.70E-04	-3.16E-04	-3.18E-06	1.67E-07	22%	37%	40%
7	OK8	Mar-93										
8	OK10	Mar-93										
9	OK8	Jul-94										
10	OK161	Mar-93	-1.19E-04	-4.65E-03	8.05E-05	-4.66E-05	2.99E-05	-5.27E-06	7.39E-09	22%	47%	31%
11	OK153	Mar-93	-3.35E-05	-2.40E-03	3.14E-05	2.18E-04	-2.05E-04	-4.81E-06	1.22E-06	8%	67%	24%
12	OK158	Mar-93	-1.68E-04	-2.37E-03	1.18E-04	-3.63E-04	-3.20E-04	7.87E-06	-3.45E-09	11%	63%	25%
13	OK168	Mar-93	-1.89E-04	-5.41E-03	2.18E-04	-3.62E-04	-3.38E-04	3.78E-06	-5.22E-09	19%	70%	10%
14	OK199bis	Mar-93	0	0	0	0	0	0	0	0%	100%	0%
15	OK158	Sep-96	-1.43E-04	-4.14E-04	1.13E-05	-1.53E-04	-1.22E-04	4.06E-06	-2.44E-09	5%	51%	44%
16	OK168	Sep-96	-1.54E-04	-3.18E-03	8.90E-05	-1.33E-04	-1.32E-04	3.88E-07	6.24E-09	14%	56%	30%
17	OK199bis	Sep-96										
18	OK0	Sep-96	3.04E-05	-5.99E-04	2.39E-06	8.63E-05	-7.86E-06	-1.31E-06	2.04E-09	19%	9%	73%
19	OK2	Sep-96	-5.89E-06	-4.87E-03	5.76E-05	5.55E-04	-2.91E-04	-2.77E-06	2.55E-08	22%	27%	51%
20	OKH2	Sep-96	-6.89E-06	4.52E-03	-8.05E-05	3.27E-04	-1.09E-05	-5.63E-07	-3.68E-09	82%	1%	17%
21	OKH3	Sep-96	4.06E-05	-3.64E-03	8.44E-05	1.65E-04	-2.31E-04	-2.48E-06	6.37E-07	18%	22%	59%
22	SA31	Sep-96	1.42E-04	-5.43E-04	-2.25E-05	3.64E-04	-9.54E-05	-1.23E-06	1.10E-08	30%	7%	63%
23	SA32	Sep-96										
24	SA34	Sep-96	4.00E-05	-2.36E-05	1.92E-06	-2.64E-05	4.04E-05	-1.03E-06	1.96E-08	14%	6%	79%
25	SA36	Sep-96	5.31E-06	-4.10E-03	3.99E-05	5.25E-04	-2.62E-04	-2.27E-06	3.90E-08	17%	24%	59%
26	SA992	Sep-96	5.84E-05	1.44E-03	-5.03E-05	3.79E-04	-1.42E-04	-1.68E-06	6.43E-07	33%	11%	56%
27	SA995	Sep-96	1.35E-04	8.77E-03	-1.68E-04	1.06E-03	-1.40E-04	-1.53E-06	2.20E-08	87%	7%	6%
28	SA996	Sep-96	1.18E-05	1.19E-03	-6.11E-05	3.33E-04	-5.74E-05	-5.43E-07	3.03E-08	34%	3%	63%
29	SA997	Sep-96	6.45E-05	4.02E-03	-9.40E-05	4.97E-04	-6.36E-05	-6.25E-07	4.17E-08	65%	1%	34%
30	pluie		0	0	0	0	0	0	0	0%	0%	100%

ISSN 1404-0344
CM Gruppen AB, Bromma, 1999